# Late Quaternary Evolution of the Northwest Nile Delta and Adjacent Coast in the Alexandria Region, Egypt

## Andrew G. Warne and Daniel Jean Stanley

Mediterranean Basin Program
U.S. National Museum of Natural History
Smithsonian Institution
Washington, DC 20560, U.S.A.

## ABSTRACT ∎

WARNE, A.G. and STANLEY, D.J., 1993. Late Quaternary evolution of the northwest Nile Delta and adjacent coast in the Alexandria region, Egypt. *Journal of Coastal Research*, 9(1), 26–64. Fort Lauderdale (Florida), ISSN 0749-0208.

The late Pleistocene to Recent evolution of the Alexandria region, Egypt, is interpreted by sedimentologic-stratigraphic study of radiocarbon-dated borings. Petrological and faunal analyses define major lithofacies, and mapping of these subsurface sequences depicts spatial and temporal distributions of sedimentary environments. Lithofacies distributions are used to compile time-slice paleogeographic maps for the past ~35,000 years. New information is provided on the origin and history (since ~6,000 years BP) of Maryut lake, the major coastal water body south and west of Alexandria. Lithostratigraphic criteria are developed to define the western limit of the Nile delta, which lies within the study area. Mapping of subsurface facies reveals that the western limit of Maryut lake (former Lake Mareotis) demarcates the western boundary of the delta; this boundary has not significantly shifted since late Pleistocene time. Facies distributions are related to natural factors which control sedimentation and coastal development in this area, and include eustatic sea-level and climatic oscillations, subsidence (compaction, isostatic depression), neotectonic uplift and sediment transport processes.

Integration of core study with geomorphic analysis serves to differentiate the impact of natural from human-induced factors. Our investigation highlights the extent to which the Alexandria region has been influenced by man, and reveals that anthropogenic factors have become a dominant control on depositional systems and coastal plain evolution. Combined effects of natural (primarily sea-level rise and neotectonism) and human-induced phenomena (e.g., wetland loss and severe pollution) are inducing changes which threaten this low-lying area. Geologic and geomorphic analyses provide information that is essential to effective coastal management of the Alexandria region.

**ADDITIONAL INDEX WORDS:** *Abu Qir lagoon, Alexandria, Carbonate ridges, Maryut lake, Neotectonism, Nile delta, Paleogeography.*

## INTRODUCTION

This study is a sedimentologic-lithostratigraphic investigation of subsurface depositional sequences of late Pleistocene to Recent age in the Alexandria region of Egypt (Figure 1). The investigation is part of a long-term geologic program, initiated at the Smithsonian Institution in 1985, to define the late Quaternary to Recent evolution of the entire northern Nile delta. Study of radiocarbon-dated sediment borings and systematic mapping of subsurface sequences are an integral part of the ongoing program to evaluate changes in the coastal region of Egypt through time. Herein, petrologic and faunal analyses serve to define major subsurface lithofacies and sedimentary environments in the study area, and core-to-core correlations of dated sections depict lithofacies distributions in time and space. A series

of time-slice paleogeographic maps are generated for the Alexandria region on the basis of these lithofacies distributions.

There have been more than 100 published studies that consider geological, geochemical, geographical and environmental aspects of the Alexandria region (many are cited in this article). Our study, however, is the first systematic and comprehensive investigation of subsurface sequences, and also the first detailed paleogeographic analysis of the Alexandria and Maryut lake region. Moreover, this study evaluates the origin and early history of Maryut lake, the major coastal water body to the south and west of Alexandria (Figure 1), and attempts to define the boundary between the delta to the east and the desert coastal plain to the west.

Comparable investigations of the late Quaternary evolution of adjacent Nile delta regions, also based largely on analysis of radiocarbon-dated sediment cores, have been carried out to the east
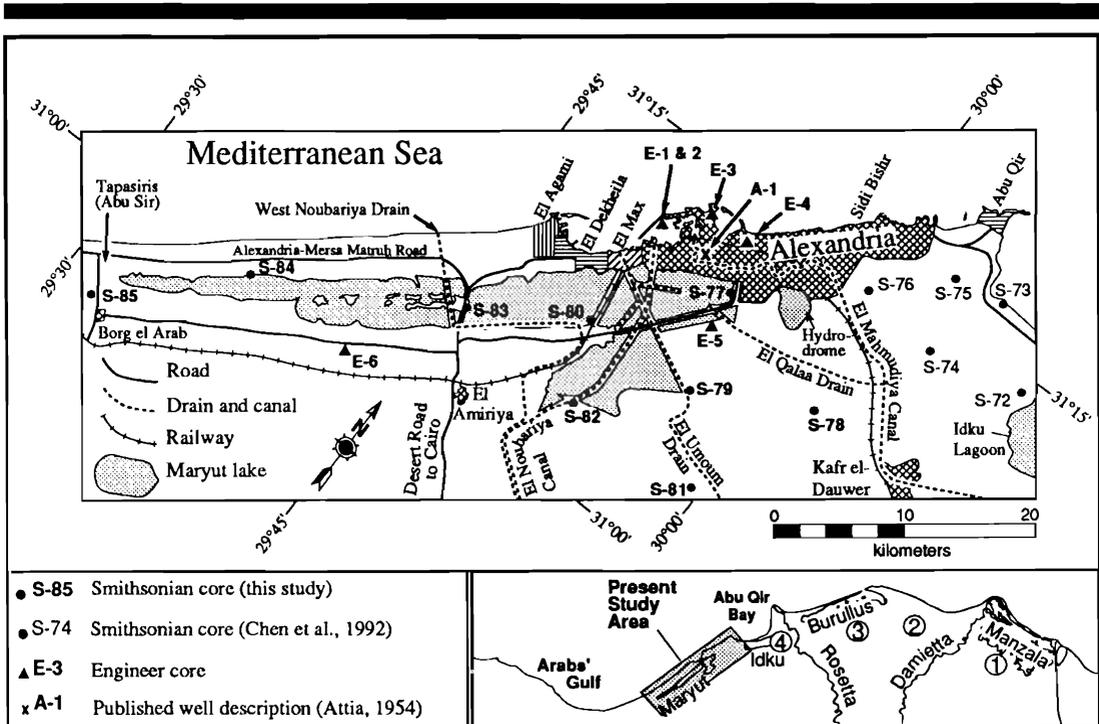
Figure 1.  Map of the Alexandria region showing prominent geographic features and position of sediment cores used in this study. Inset map demarcates general locations of comparable Smithsonian Nile Delta Project studies to the east: (1) Coutellier and Stanley (1987), (2) Stanley et al. (1992), (3) Arbouille and Stanley (1991), and (4) Chen et al. (1992).

(COUTELLIER and STANLEY, 1987; ARBOUILLE and STANLEY, 1991; STANLEY et al., 1992; CHEN et al., 1992). These companion studies (Figure 1, inset) have demonstrated that, as in the case of most delta shorelines (cf. BROUSSARD, 1975; COLEMAN, 1982), modifications in the northern Egypt coast through time have been induced by eustatic sea-level and climatic oscillations, subsidence (compaction, isostatic depression, neotectonism) and sediment transport processes. Previous studies have shown that, in addition to these natural phenomena, man has affected profound physiographic and ecologic transformations on the northern Egypt coast. Anthropogenic alterations include land reclamation, agricultural, aquacultural, irrigation and industrial projects (BUTZER, 1976; WATERBURY, 1979).

In addition to interpretation of the late Quaternary evolution of the Alexandria region, the major goal of the present investigation is to provide necessary data to monitor ongoing and future changes in the northern coastal region of Egypt. Alexandria, highly industrialized and Egypt's largest port, must come to terms with exponential

population growth and severe pollution (cf. EL-WAKEEL and WAHBY, 1970; EL-WAKEEL and EL-SAYED, 1978; SAAD, 1983a,b; EL-RAYIS et al., 1986; ELSOKKARY, 1989; and ABOUL DAHAB et al., 1990). Interpretation of radiocarbon-dated cores provides the most effective means to differentiate the effects of natural from human-induced factors that control lithofacies distribution and coastal development. Our analysis was initated to provide vital information for preparation and implementation of effective plans to help protect and remediate the low-lying Alexandria region.

## METHODOLOGY

Fourteen Smithsonian sediment cores, collected during a 1990 field expedition (Figure 1), were analyzed in this study. These 7.5 cm diameter cores, recovered using a trailer-mounted rotary percussion (Acker-2) drilling rig, range in length from 10 to 45 m and are spaced ~4 to 16 km apart. Cores were collected as continuous sections where sediment was cohesive, and as washings (by circulating water) where sandy and noncohesive. Nine of these cores (S-77 to S-85) were analyzed

during the course of this study (Figure 1); the other five cores (S-72 to S-76) were examined in a previous investigation (CHEN et al., 1992). In addition, lithologic logs of six engineering borings (E-1 to E-6) and one published log (A-1 in ATTIA, 1954) are incorporated into the subsurface database. Moreover, other published lithologic logs (FOURTAU, 1896, 1915; ATTIA, 1954; SAID, 1981; SESTINI, 1989) were consulted for this study.

Each Smithsonian core was systematically split and macroscopic features such as general lithology and color, hardness, stratal boundaries, sedimentary structures, fossil content, root traces and other features were recorded. All core sections were x-radiographed for detailed examination of sedimentary structures and traces of plants and organisms (cf. method of COUTELLIER and STANLEY, 1987). From the fourteen cores, 444 samples were collected for petrographic analysis at each lithological boundary, or at less than 1 m intervals in the case of thick homogeneous sections. An additional 47 samples were radiocarbon dated (using total organic matter, plants and/or shell); of these, 31 provided viable ages to establish a chronostratigraphic framework.

Size analysis was performed on the 444 petrologic samples to determine proportions of clay (<2 $\mu$m), silt (2–63 $\mu$m) and sand (>63 $\mu$m). The average size (very fine, fine, medium, coarse, very coarse) of the sand fraction was determined for all samples by comparing these samples (under a reflected light microscope) to sand-size standards in a Grain Sizing Folder (©Forestry Suppliers Inc.). Such sand-size analysis has proved to be particularly useful to differentiate marine-influenced lagoon from brackish water bay deposits (cf. CHEN et al., 1992).

Petrographic analysis (cf. method of COUTELLIER and STANLEY, 1987) of the sand-size fraction was used to distinguish the major sedimentary facies. Relative percentages of 18 sand-size components were calculated from point counts of >300 grains for the 444 samples (method of FRIHY and STANLEY, 1988). Counted components include: 9 mineralogical (light and heavy mineral, mica, verdine/glauconite, pyrite, gypsum, lithic fragment, undefined carbonate particle and carbonate aggregate); 6 faunal (indeterminate shell fragments, foraminifera, ostracod, gastropod, pelecypod and sponge); and 3 floral (diatom, plant fragment and seed). This method is particularly useful for differentiating (1) late Pleistocene siliciclastic alluvial plain sands, deltaic siliciclastic to coastal carbonate sands, and carbonate desert coastal sands; and (2) Holocene fluvially-influenced and marine-influenced lagoon deposits.

Distinct molluscan fossil assemblages have been shown to be representative of specific range of marine conditions and water depths in the Mediterranean region (DI GERONIMO and ROBBA, 1976), including the Nile delta (BERNASCONI et al., 1991). In this study, molluscan paleocommunity analysis was performed (M.P. BERNASCONI, written communications, 1991, 1992) on 24 samples from nine cores (S-73, S-75, S-77, S-78, S-79, S-80, S-82, S-83, S-84) to more precisely define the environments of deposition for the sampled intervals. Paleocommunity analysis is particularly useful in differentiating among brackish water bay, marine-influenced lagoon and fluvially-influenced lagoon facies.

Following the procedure described above, the various late Quaternary lithofacies were distinguished for each boring. Core-to-core correlations were then established, taking into account available radiocarbon ages. These correlations highlight lithofacies distributions (and associated environments of deposition) in time and space. A series of time-slice paleogeographic maps, based primarily on facies distributions, was then compiled. All relevant information is recorded in MEDIBA (1992).

A generalized geomorphic-land use map (Figure 2) of the Alexandria region was compiled to better relate present-day sedimentary environments to sub-recent and modern coastal processes, and also to record the profound impact of man on this densely populated and highly industrialized region. This map was compiled primarily from Landsat-5 Satellite Thematic Mapper images (bands 3, 4, 5, 7) which were taken during a survey in December, 1986, and published by IWACO (1989; scale 1:100,000). Additional information was obtained from topographic (U.S. DEFENSE MAPPING AGENCY, 1961, 1973, 1975, 1977; scale 1:50,000) and other pertinent maps (ARROWSMITH, 1802, 1807; JACOTIN, 1818; SHATA, 1958; EL-SAMI, 1960; EL FAYOUMY et al., 1975; FRIHY et al., 1988; CHEN et al., 1992). Geomorphologic features of the Alexandria region were observed during 1990 and 1992 Smithsonian field expeditions.

Bathymetric (Figure 3) and topographic (Figure 4) maps of the region were compiled to better characterize the sedimentary and tectonic settings of this region which comprises the transition
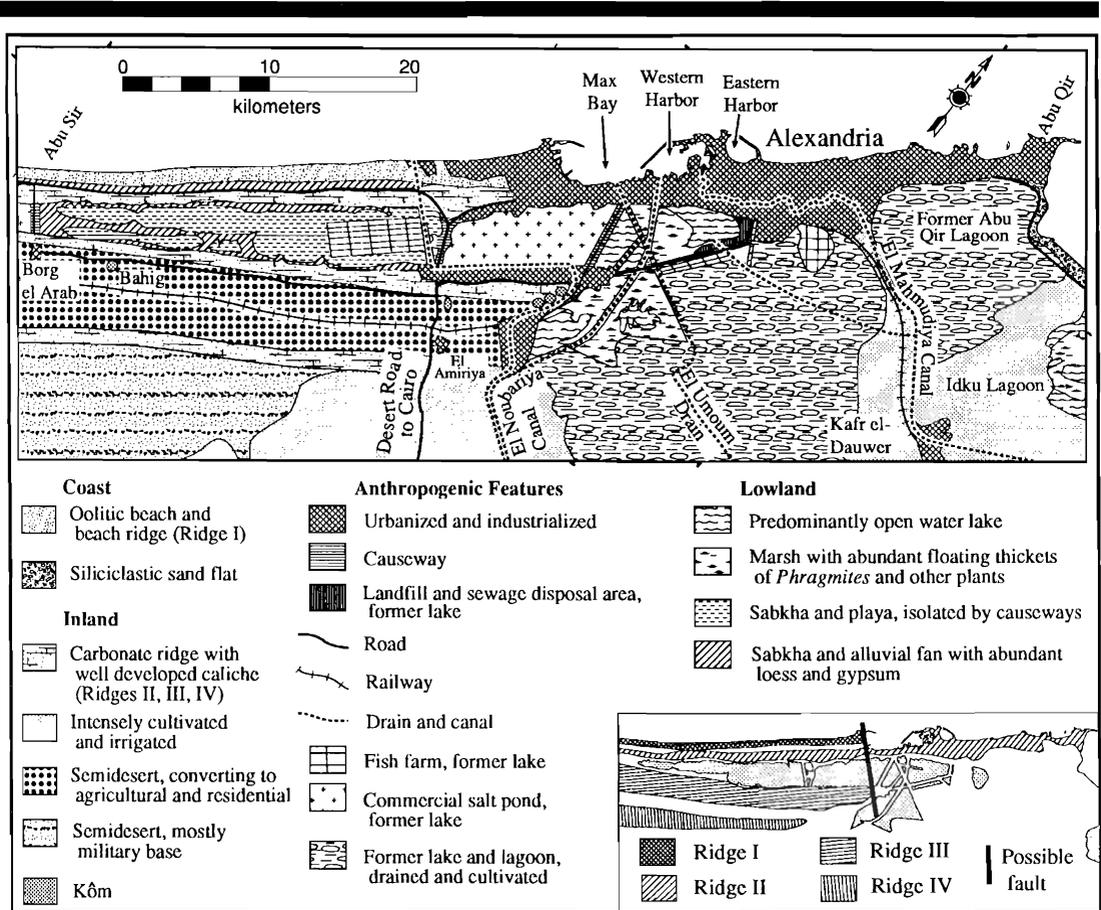
Figure 2. Geomorphic-land use map of the study area. Primary source of data is Landsat-5 Satellite Thematic Mapper images taken in a December 1986 survey (IWACO, 1989). Diversity of geomorphic features reflects (1) the transition from Nile delta plain to the east and desert coastal plain to the west, and (2) profound influence of human activity. Descriptions of various geomorphic features is given in text. Inset map shows eastern portions of late Pleistocene carbonate ridges, and position of possible fault (Butzer, 1960).

from deltaic to desert littoral environment. These maps were compiled from documents of the U.S. DEFENSE MAPPING AGENCY (1961, 1973, 1975, 1977, 1985, 1990; scale 1:50,000) and SHAFEI (1952).

## DESCRIPTION OF THE STUDY AREA

The study area parallels the SW-NE oriented coast for a distance of ~70 km, and extends ~20 km inland. It is located at the western edge of the Abu Qir Bay and includes the northwestern sector of the Nile delta (HILMY, 1951; SHUKRI and PHILLIP, 1956; STANLEY and HAMZA, 1992). This coastal region lies at the eastern end of Arabs' Gulf (Figure 1, inset) and includes the eastern portion of the Western Desert coastal zone. The Alex-

andria region can be subdivided into a series of distinct geomorphic areas, including beach, carbonate ridge, inland depression, drain and canal, kôm (low hill), semidesert, reclaimed lagoon and irrigated farmland. The coastline between Abu Qir and El Dekheila is characterized by alternating small bays and pocket beaches which are separated by headland points and small islands (SHUKRI and PHILLIP, 1956). In contrast, the coast from El Dekheila to Abu Sir (and further west) is characterized by broad white, carbonate beaches. Maryut lake, a shallow brackish water body with no direct connection to the sea has been artificially divided into >9 sub-basins by causeways and canals, and is heavily polluted by un-
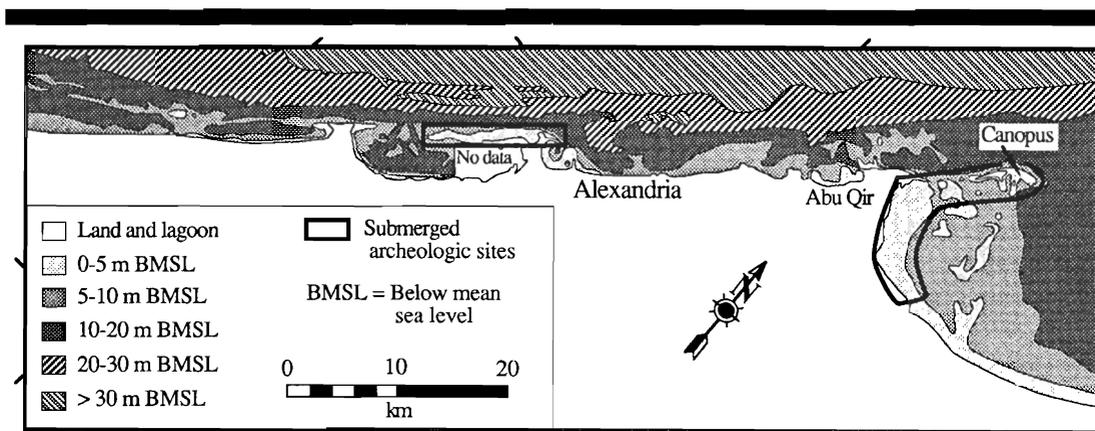
Figure 3.   Bathymetric map of the Alexandria nearshore region. Primary source of data is U.S. Defense Mapping Agency (1985, 1990). Submerged features and archeological sites are discussed in text.

treated sewage and industrial wastes. Other distinctive geomorphic features of the study area include a series of shore-parallel carbonate ridges (to >40 m elevation); these are separated by depressions which contain shallow lagoons and sabkhas. Large portions of the study area lie below sea level (Figure 4) and thus are particularly vulnerable to marine inundation.

The Alexandria region has a long record of human habitation, dating back to pre-dynastic times. By 5,000 years BP, herdsmen had migrated to the Mediterranean coast as the climate of western Egypt became more arid and the former grasslands converted to desert (DE COSSON, 1935; BUTZER, 1976). The earliest historical record dates back to ~3400 BC when the region was known as Kingdom of the Harpoon (the harpoon was used for catching fish in Lake Mareotis). Historic records indicate that Lake Mareotis (predecessor of Maryut lake) was a fresh water lake, which was deeper and of greater aerial extent than at present (DE COSSON, 1935). The history of Lake Mareotis is discussed in more detail in a later section.

### Marine Shelf

The nearshore marine shelf is primarily composed of sand which is fine and siliciclastic in the east, and coarse and carbonate-rich in the west (EL-WAKEEL and EL-SAYED, 1976, 1978; EL-SAYED, 1979, 1988c). Textures grade from sand near the coast to muddy silt 5–8 km offshore (EL WAKEEL and EL-SAYED, 1978, their Figure 3). The middle shelf is primarily composed of skeletal and pelloidal carbonate sand and mud (SUMMERHAYES et

al., 1978; STOFFERS et al., 1980). Several small islands, remnants of a carbonate ridge, dot the nearshore between Abu Qir and El Agami (EL-SAYED, 1988a). BUTZER (1960) and EL-WAKEEL and EL-SAYED (1978) described a series of bathymetric highs ~1–1.5 km offshore that parallel the present shoreline. EL-WAKEEL and EL-SAYED (1978) considered these to mark an ancient shoreline which has subsided below sea level. At a resolution of 5 m, the bathymetry shown in Figure 3 does not reveal this submarine feature. Sediments along the coast are polluted by untreated seawater, industrial waste and contamination related to the shipping industry (ABDEL-MOATI and EL-SAMMAK, 1988; ABOUL DAHAB, 1988).

Oolites of Arabs' Gulf have been interpreted by some to be relict sediments which formed during warmer periods of the late Quaternary (ANWAR et al., 1981). Petrographic analysis by ALEXANDERSSON (1990), however, suggests that oolization may be in progress at present.

### Coastal Area

The coast, especially at Alexandria and El Agami, is the principal seaside resort in Egypt, seasonally attracting millions of vacationers. Complete modification of segments of the coastline, from Alexandria to El Agami, has resulted from rapid construction to house the fast-growing population and to accommodate industry and shipping at Egypt's principal port.

On the basis of geomorphology and sedimentology, the coast from western Abu Qir bay to the
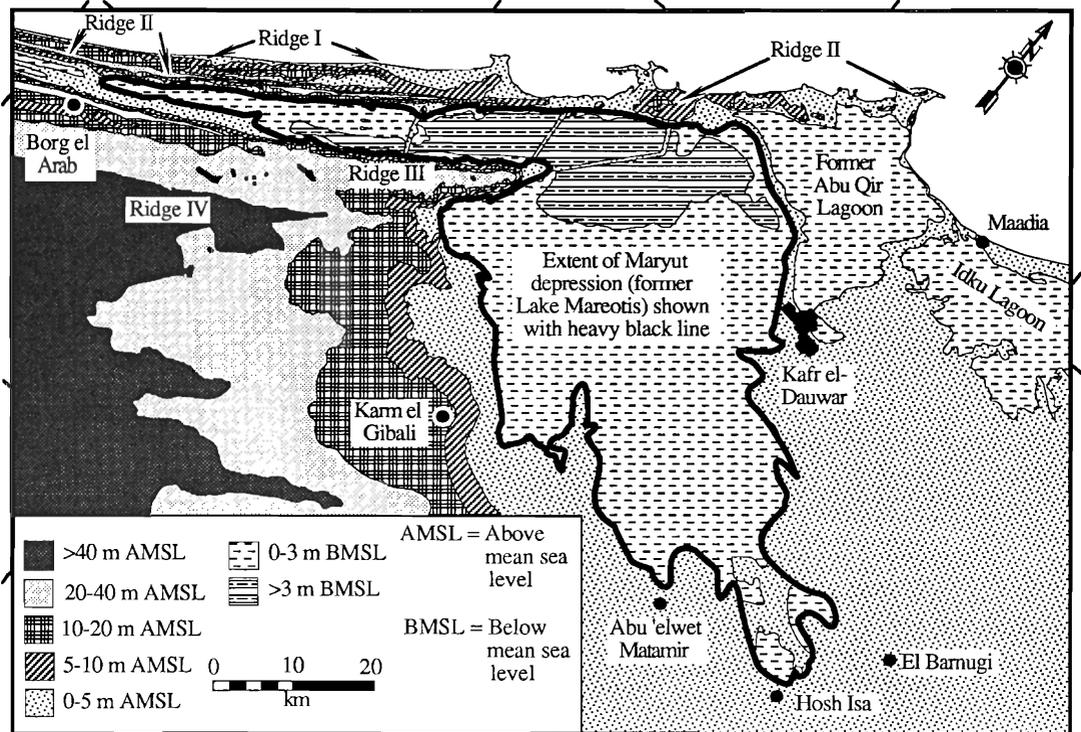
Figure 4. Topographic map of the Alexandria region. Primary source of data is U.S. Defense Mapping Agency (1961, 1973, 1975, 1977). This map highlights (1) the large land surface below sea level, including former Lake Mareotis, and (2) physiographic expression of the transition between the low-lying Nile delta plain to the east and carbonate ridges of the coastal plain to the west. Topographic features are discussed in text.

ruins at Tapasiris (Abu Sir) can be subdivided into four zones: western Abu Qir bay; Abu Qir–El Dekheila coast; Alexandria harbor district; and El Dekheila–Tapasiris coast (cf. HILMY, 1951; SHUKRI and PHILLIP, 1955; PHILLIP, 1976; EL-WAKEEL and EL-SAYED, 1978). These four coastal zones are described below, from east to west.

The siliciclastic beach and sand flat south of Abu Qir extends for ~7 km along the westernmost portion of Abu Qir bay (Figure 2). This coastal sector is primarily composed of very fine to medium quartz sand (CHEN et al., 1992). Micas, heavy minerals and mollusc shells are common accessory components. The relative proportion of carbonate increases northward towards the carbonate ridge at Abu Qir. The sand flats are generally <1 m above mean sea level, but intermittent dunes reach 2 m in elevation (EL FAYOUMY et al., 1975). These low-lying sand flats extend 0.5–0.75 km inland.

The 30 km of coastline between Abu Qir and El Dekheila is characterized by small bays separated by capes and small islands (Figure 5A). Sea cliffs (to ~5 m) are common along this coast and form as waves erode carbonate coastal ridges. Along this portion of the coast, sandy beaches are generally narrow and are best developed in small bays (Figure 5A). Many of these beaches are now artificially replenished with sand. Carbonate content, mostly in the form of shell and shell fragments, increases markedly westward, from ~36% at Abu Qir to ~99% at El Dekheila (HILMY, 1951). In contrast, proportions of quartz and heavy minerals decline westward, reflecting the diminished influence of the River Nile on this geomorphic province (HILMY, 1951; SHUKRI and PHILLIP, 1955). The sands from Abu Qir to Sidi Bishr (Figure 1) are generally fine to medium, whereas the sands from Sidi Bishr to El Dekheila are generally coarse (EL-WAKEEL and EL-SAYED, 1978). The boundary

Figure 5. Photographs of selected geomorphic and sedimentologic features in the study area. (A) carbonate Ridge II forming small cape and pocket beach at Muntazah park, between Alexandria and Abu Qir (view toward north). (B) roadcut through Ridge II between Borg el Arab and coast, near Abu Sir (Tapasiris); elevation of ridge crest ~35 m (view northwest toward Arabs' Gulf). (C) Ridge II quarried for building stone at Sidi Barakat, southwest of Alexandria; note large-scale bedding (ridge crest ~30 m). (D) Mallahet Maryut depression between Ridge II (Tapasiris archeologic site in foreground) and Ridge III in distance (view toward southwest). (E) driller at core site S-85 (between Ridges II and III) near Borg el Arab, recovering carbonate sands which produce characteristically white drilling fluids. (F) cultivated field in former Abu Qir lagoon near Abu Qir bay coast; note date palms on raised sand barrier (view toward east). (G) view of El Umoum drain, which traverses and subdivides Maryut lake (view from Desert road toward southeast). (H) causeway traversing southwestern sub-basin of Maryut lake, near core site S-82; carbonate Ridge III in background (view toward west). (I) commercial salt pond (crusts in white) in west-central sub-basin near core site S-83; factories of western El Agami in background (view toward northeast).
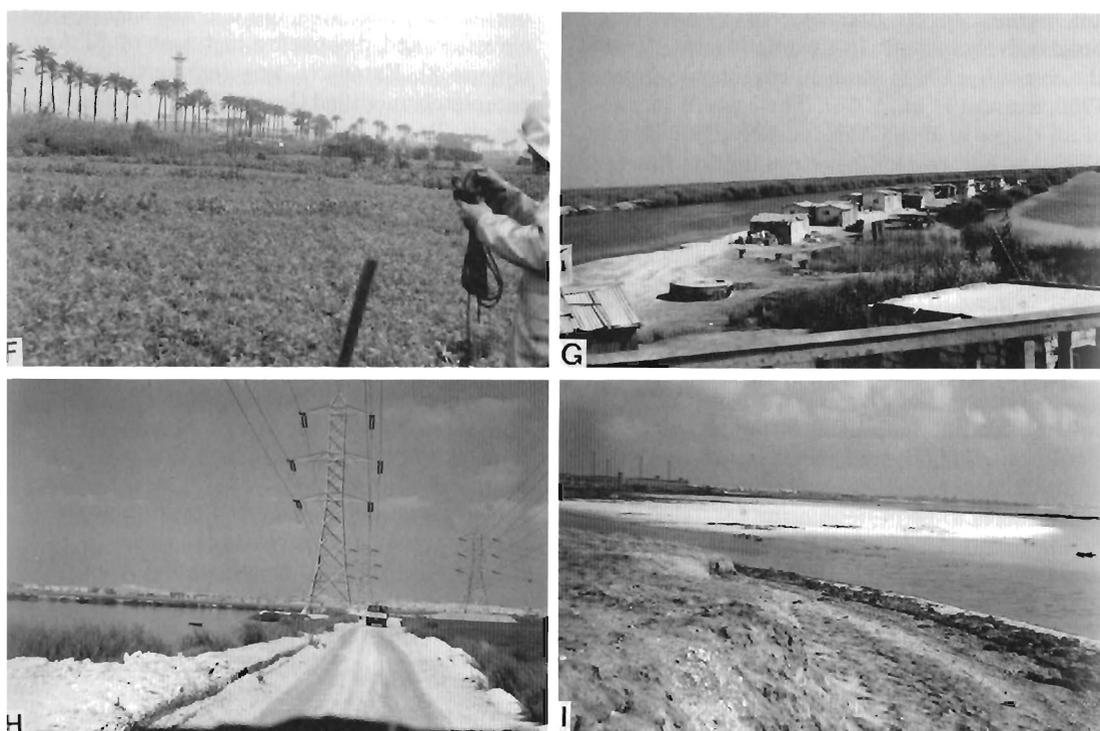
Figure 5. Continued.

between the Nile delta and the Western Desert coast occurs in this region (STANLEY, 1989, his Figure 4).

There are two principal harbors along the Alexandria coast: the Eastern and Western harbors (Figure 2). These two adjacent harbors are protected from the sea to the north by remnants of a limestone ridge (formerly Pharos Island) and man-made jetties. The two harbors were once a single water body, but were divided by a causeway which was constructed by order of Alexander the Great (JONDET, 1916; MORCOS, 1985). The Western harbor covers ~31 km² and has an average depth of ~7 m. This harbor handles ~90% of the foreign trade of Egypt. Because it is a semiclosed basin, the only significant sediment source is untreated sewage and industrial waste (EL-SAYED et al., 1988). The harbor bottom is covered by highly polluted, dark gray to black, organic-rich mud (EL-WAKEEL and EL-SAYED, 1978). The Eastern harbor covers ~25 km² and averages ~6 m in depth. This semiclosed basin is covered by grayish black to black sandy silts (EL-WAKEEL, 1964) and currently receives large volumes of untreated sew-

age (DOWIDAR and ABOUL KASSIM, 1986; EL-RAYIS et al., 1986).

In contrast to the irregular coastline in the northeastern study area, the 40 km stretch from El Dekheila to Tapasiris is characterized by straight, carbonate-rich sandy beaches of variable width. These beaches are backed by dune ridges which, in their natural state, are driven landward by dominant southeast-directed winds. The sands along this stretch of coast are medium-grained, well sorted and well rounded (HILMY, 1951). The carbonate content is high (>99%) whereas quartz and heavy minerals are found only in trace amounts; the heavy minerals generally comprise the more stable varieties (SHUKRI and PHILLIP, 1955; EL-WAKEEL and EL-SAYED, 1978). Ooids and coated grains make up 85% of the carbonate fraction; shells and shell fragments constitute most of the remainder (STANLEY and HAMZA, 1992).

### Carbonate Ridges

The western portion of the study area is characterized by a series (perhaps as many as 8–10) of elevated carbonate ridges of late Pleistocene

age. These ridges extend westward, some for > 100 km, parallel to the present coast. These ridges progressively increase in elevation from ~10 m at the coast to ~100 m some 40 km inland (ZEUNER, 1950; SHUKRI et al., 1956). The eastern terminus of all ridges is in the Alexandria region (BUTZER, 1960, his Figure 1). Their termination has been attributed to downwarping under the weight of the Nile delta sediment load (HASSOUBA, 1980; cf. SAID, 1981), and faulting (BUTZER, 1960).

There are several interpretations as to environment of deposition of the late Pleistocene ridges: some studies concluded that the three northernmost ridges are shallow marine deposits such as offshore bars (FOURTAU, 1893; BLACKENTHORN, 1901, 1921; ZEUNER, 1952; SHUKRI et al., 1956; SAID et al., 1956; BUTZER, 1960; ISMAIL and SELIM, 1969; CHERIF et al., 1988), whereas others consider these ridges to be of nonmarine coastal dune origin (HUME, 1912; HUME and HUGHES, 1921; HUME and LITTLE, 1928; BALL, 1939; SANDFORD and AR-KELL, 1939; PICARD, 1943; SCHWEGLER, 1948; HILMY, 1951; PAVER and PRETORIUS, 1954; SHATA, 1955). However, in light of evidence from a recent trench across a ridge near Bahig (Figure 2), some authors concluded that this ridge is of both marine and eolian origin (HASSOUBA, 1980; HASSAN et al., 1986). It has been suggested that the elevation of carbonate ridges records successive late Pleistocene sea level stands (SHUKRI et al., 1956; HASSAN et al., 1986). However, some studies conclude that, over time, these and related carbonate ridges around the Mediterranean Sea have been elevated by tectonic processes (EL RAMLY, 1968; HEY, 1978; NEEV et al., 1987).

In the present study, the three northernmost ridges are termed Coastal Ridge I, Abu Sir Ridge II and Gebel Maryut Ridge III (Figure 2, inset), and are briefly described below.

### Coastal Ridge I

Coastal Ridge I parallels the shore from Alexandria westward to about 30 km east of the Libyan border. Along its entire extent, the carbonate content exceeds 98.5% and is classified as an ooid grainstone (STANLEY and HAMZA, 1992). Accessory components include fossils of algae, molluscs, foraminifera and micritic carbonate particles; quartz is rare to absent. Ridge I is commonly cross-laminated, in which foresets trend dominantly to the southeast. Coastal Ridge I is composed of white, well sorted, medium-grained, loose to lightly cemented, carbonate sands. This ridge is as much as 10 m above mean sea level in the western part of the study area, but decreases markedly in elevation and disappears just east of El Agami (Figure 2). Extensive, ongoing construction has completely modified Coastal Ridge I in the Agami region. To the west, where undisturbed by man, the upper surface is partially covered by coastal and dune plants, and is fronted by beaches of variable widths which are also composed of white oolitic sands. These back-beach dunes are displaced by dominant southeast directed winds, and thus are migrating to the southeast. In places, these coastal dune sands have infilled the depression between Ridges I and II, resulting in a series of discontinuous sabkhas and playas.

Oolitic sands in the upper portion of Coastal Ridge I are interpreted to have originally formed on the shelf in Arabs' Gulf. These shallow shelf sands were then transported onto the beach by marine waves and currents, and then onto the ridge by southeast-directed winds. A late Monasterian age has been attributed to these deposits (SHUKRI et al., 1956; CHERIF et al., 1988).

### Abu Sir Ridge II

Abu Sir Ridge II is almost parallel to and landward of Coastal Ridge I (Figure 2, inset), and extends from Abu Qir westward to the town of El Sallum, near the Egyptian-Libyan border. Abu Sir Ridge II limestones have been classified as mostly ooid-coated grain-bioclastic grainstones (STANLEY and HAMZA, 1992). The relative proportion of quartz and other insoluble residue is very high in the northeast (~76%) but decreases markedly to the southwest (STANLEY and HAMZA, 1992). Allochems are primarily ooids, coated grains and algae (STANLEY and HAMZA, 1992). In the walls of quarries, these grainstones commonly display high angle, unidirectional (to the southeast), large-scale, planar cross bedding. Thin calcrete crusts (2–15 cm thick) occur irregularly throughout the ridge sequence; these suggest intermittent subaerial exposure of the ridge deposits and subsequent meteoric diagenesis (EL-SHAHAT et al., 1987). The elevation of this cream colored limestone ridge averages about 35 m in the western part of the study area (Figure 5B), and decreases eastward to 6 m at Abu Qir. The city of Alexandria is built upon this ridge. It is quarried in the western part of the study area, primarily for building stone and cement (Figure 5C). In the western portion of the study area there is little soil or vegetation along the ridge crest, and a caliche crust is

well developed. Flanking both sides of the ridge are extensive alluvial fans of poorly sorted, weathered Ridge II sediment. This ridge has been assigned a "main Monasterian" age in some studies (BLACKENHORN, 1921; SHUKRI et al., 1956; CHERIF, 1988).

### Gebel Maryut Ridge III

Gebel Maryut Ridge III lies south of, and parallel to Abu Sir Ridge II. In the study area these two ridges are separated by a 3 to 4 km-wide depression occupied, in part, by the western extension of Maryut lake. The yellow to light-brown Ridge III changes from mostly quartz-rich carbonate sandstones in the northeast to mostly bioclastic grainstones in the southwest (STANLEY and HAMZA, 1992). Ridge III is fossil-rich and characterized by a diverse faunal content (STANLEY and HAMZA, 1992). True ooids are absent. The elevation of Gebel Maryut Ridge III ranges from 20 to 40 m. As in the case of Ridge II, there is little soil or vegetal cover along the crest, and a caliche crust is well developed. Flanking both sides of the ridge are extensive alluvial fans of poorly sorted Ridge III sediment.

Studies of a large trench cut across Ridge III near Bahig (Figure 2) have lead recent workers to conclude that this ridge formed under a wide variety of conditions ranging from marine to eolian (HASSOUBA, 1980; HASSAN et al., 1988; STANLEY and HAMZA, 1992). Several well developed paleosols are interbedded with Ridge III marine carbonates; these interbedded marine and subaerial deposits record several cycles of submergence and emergence during the course of ridge development (HASSAN et al., 1986). Previous studies have assigned a late Tyrrhenian age to these deposits (SANDFORD and ARKELL, 1939; SHUKRI et al., 1956; CHERIF et al., 1988).

### Inter-ridge Depressions

The shore-parallel carbonate ridges are separated by a series of elongate depressions. The floor of successive depressions increases in elevation to the south (Figure 4). The depressions are generally covered by brown, calcareous clayey loess (HASSOUBA, 1980; ALI and WEST, 1983). Beneath the loessic cover are calcareous and gypsiferous clayey silts which have been interpreted to have accumulated in shallow lagoons and sabkhas (SAID et al., 1956; HASSOUBA, 1980; HASSOUBA and SHAW, 1980). These sediments are locally mined for gypsum to the south and west of the study area. Vadose gypsum nodules are currently forming in the two northernmost depressions (Depressions I and II of ALI and WEST, 1983). These two northernmost depressions are briefly discussed below.

### El Dekheila-Abu Sir Depression I

The El Dekheila-Abu Sir Depression I between Coastal Ridge I and Abu Sir Ridge II, is narrow (0–0.5 km) and discontinuous. In places, Coastal Ridge I has expanded southeastward and infilled Depression I, which has resulted in a series of isolated playas and sabkhas. The upper 1 to 2 m of Depression I sediment consists of ooid-bearing calcareous silt (loess) with abundant gypsum nodules. These nodules are forming at the present time (WEST et al., 1979; HASSOUBA, 1980; ALI and WEST, 1983). These gypsiferous silts are underlain by gray shelly silts of lagoon origin (ALI and WEST, 1983). The sabkha surface is 0 to 1 m above sea level. The surface is flat and partially vegetated with halophytic shrubs. In summer the surface is dry and capped by a 2 mm crust of silt cemented by halite and gypsum (ALI and WEST, 1983). In winter (depending on the amount of rainfall) the depression is partially filled with water. Just west of El Agami, sectors of this depression have been artificially infilled (with Ridge I sands) for commercial and residential use.

### Mallahet Maryut Depression II

The Mallahet Depression II, situated between Abu Sir Ridge II and Gebel Maryut Ridge III, is continuous and generally between 3–4 km wide (Figure 5D and E). The surface of this depression descends to more than 3 m below sea level (Figures 2, 4). Until the twelfth century, AD, this depression served as the western branch of Lake Mareotis (DE COSSON, 1935). Presently, Depression II is artificially segmented into several subbasins by causeways and canals (Figure 2). Mallahet Maryut Depression II is discussed further in association with the Maryut depression.

### Maryut Depression

Maryut, which covers ~90 km², is presently the smallest Nile delta coastal brackish water body (Figure 2). Unlike the other three Nile delta lagoons, Maryut has no direct connection to the sea, and therefore is herein referred to as Maryut lake (as opposed to Maryut lagoon). Maryut lake surface is currently maintained at 2.8 m below mean sea level by pumping water from the lake to the sea at El Max. With present water depths up to

1.5 m and lake levels at 2.8 m below sea level, the floor of Maryut lake extends to as much as 4.3 m below sea level, appreciably lower (by nearly 3 m) than other northern Nile delta lagoons.

Because of the artificially low lake levels, Maryut lake occupies a fraction (~13%) of an extensive subsea-level depression which is herein referred to as Maryut depression (Figure 4). The remaining 87% of the depression has been drained and is now used primarily for agriculture (Figure 2). Modern Maryut lake, subdivided into more than nine sub-basins by causeways and canals (Figures 5G and H, 6), is heavily polluted and partially eutrophic. Maryut lake and its predecessor, Lake Mareotis, will be discussed in detail in a later section.

### Former Abu Qir Lagoon

Former Abu Qir lagoon occupied ~105 km² in the region just east of Alexandria and south of Abu Qir city (Figures 2, 5F). This low-lying region was wetland until as late as the early nineteenth century (ARROWSMITH, 1802, 1803; JACOTIN, 1818; FOURTAU, 1896). Although drained and intensely cultivated, the former lagoon is still discernable on satellite images. The eastern margin of this subsea-level depression is separated from the coast by narrow (0.5–0.75 km) coastal sand flats (Figures 2, 4, 5F).

### Canals and Drains

An extensive network of irrigation canals covers large portions of the southeastern sector of the study area (U.S. DEFENSE MAPPING AGENCY, 1961, 1975, 1977). The southwestern portion of the area is less extensively cultivated, but irrigation projects are expanding into that region. El Mahmudiya, El Qalaa, El Umoum, El Noubariya and West Noubariya canals and drains, the principal inland waterways in the study area, are briefly discussed below (Figures 1, 2).

To the east of the study area, El Mahmudiya canal follows the course of the former Canopic channel, once a major distributary of the River Nile (TOUSSON, 1992; CHEN et al., 1992). Even before the arrival of Alexander the Great in 332 BC, El Mahmudiya canal (formerly the Alexandria canal) had been constructed to supply small villages of the region with drinking, bathing and irrigation water (DE COSSON, 1935). When the Canopic channel silted up in the twelfth century, El Mahmudiya canal was extended to the Rosetta branch. However, the canal silted up during the

same century and Alexandria declined in importance. El Mahmudiya canal was rebuilt by Mohamid Ali Pasha in 1820 and once again Alexandria became a principal city of Egypt. The canal currently supplies the Hydrodrome with water. The course of the El Mahmudiya canal through downtown Alexandria is now dry, although it is still recognizable on satellite images (Figures 1, 2).

El Qalaa drain is a branch of El Mahmudiya canal and receives large amounts of industrial wastes from the Alexandria region. It is the principal source of water (and also pollutants) for Maryut lake.

El Umoum drain receives agricultural runoff from the Beheirah Governate (Figure 5G). Its waters are less polluted than those of El Qalaa drain (EL-RAYIS and SAAD, 1986). A series of breaks along its embankments allows the canal water to mix with that of Maryut lake. Water is pumped from this drain at El Max to maintain Maryut lake at 2.8 m below sea level (ALEEM and SAMAAN, 1969a).

El Noubariya canal is the major water way in the westernmost Nile delta, and serves as a principal artery for shipping barges in the Alexandria region. The canal has been polluted with tin from antifouling agents used in paints which are applied to barges using this canal (ABOUL DAHAB et al., 1990). The West Noubariya canal, more recently constructed, is also used for barge traffic.

### Kôms and Tells

Several hills, referred to as kôms or tells, are conspicuous features in the depression between carbonate Ridges III and IV and are readily recognized on aerial photographs and satellite images (Figure 2). These hills, largely composed of fine and medium sand and silt, characteristically contain abundant artifacts which have proven to be of great value to archeologists working in this region (RODZIEWICZ, 1984). DE COSSON (1935) described the two kôms near Bahig (Figure 2) as "artificial mounds".

### Arable Lands

Low-lying arable lands of the study area make up the northwestern sector of the fertile Nile crescent. Construction of the Aswan High dam in 1964 brought an end to annual floods in the delta, and to the influx of large volumes of nutrient-rich sediments carried by the flood waters (SHARAF EL DIN, 1977). These sediments were not only im-
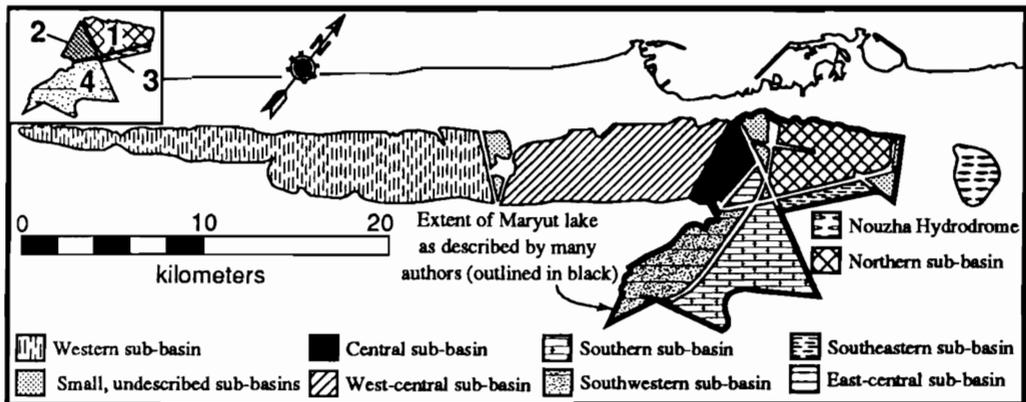
Figure 6. Map showing artificial sub-basins of present-day Maryut lake. Sub-basins are separated by canal embankments and causeways. Inset map shows four Maryut sub-basins as described by several authors (*cf.* Aleem and Samaan, 1969a).

portant for keeping the soil nutrient rich, but also for maintaining the balance between sediment input, land subsidence and sea-level rise. Without sediment input, ongoing sea level rise and subsidence will make the region vulnerable to inundation by the sea. The study area is especially at risk because large portions of the arable land are reclaimed lake and lagoon which already lie below sea level (Figures 2, 4). Therefore, significant increase in sea-level rise or subsidence, or breaching of the coastal barriers by winter storms or earthquakes, may result in inundation of coastal regions by the sea.

**Depositional Processes Affecting the Alexandria Region**

UNDP/UNESCO (1976, 1977, 1978), INMAN and JENKINS (1984), STANLEY et al. (1992) and CHEN et al. (1992) have described the climatic, fluvial and marine conditions influencing the northern Nile delta. Winds are predominantly southeast-directed (NAFAS et al., 1991). Wind speeds are generally between 2 and 50 km per hour. Wind storms (known as "khamsin") most commonly take place from January to April and have been shown to be effective in transporting large volumes of dust in this region (OLIVER, 1945, 1946).

The Alexandria region receives an average of 200 mm of rainfall per year, but precipitation varies greatly from year to year. Rains are seasonal: almost all rain occurs between December through February, whereas between June and August there is essentially none. Annual evaporation potentials of 1.5 m far exceed precipitation. DE COSSON (1935)

suggested that climate in the region has become drier during the past 1,200 years, although variations have been reported (BELL, 1970; HASSAN, 1981; RIEHL and MEITIN, 1979). The Alexandria coastline is microtidal along which waves, approaching from the northwest, drive marine currents and sediments to the east and northeast. These marine currents prevent Nile siliciclastics from reaching further west than the shores of eastern Alexandria (STANLEY, 1989). It should be recalled that, until recently (closure of Aswan High dam), large volumes of Nile sediments debouched at nearby Rosetta promontory.

**DESCRIPTION AND INTERPRETATION OF LATE QUATERNARY FACIES**

Subsurface lithofacies in this westernmost Nile delta sector were distinguished and interpreted by macroscopic observations of split core sections and by petrographic analyses on the sand-size fraction of core samples (*cf.* methods of COUTELLIER and STANLEY, 1987). Interpretation of depositional environments associated with these facies was refined by identification of molluscan paleocommunities (*cf.* BERNASCONI et al., 1991; M.P. BERNASCONI, *written communications*, 1991, 1992), and by combined compositional and stained grain analysis (*cf.* STANLEY and CHEN, 1991).

A synthesis of vertical and lateral facies relationships is presented in Figure 7. Most lithofacies described below have been discussed in previous Nile delta studies (COUTELLIER and STANLEY, 1987; ARBOUILLE and STANLEY, 1991; STANLEY et al., 1992; CHEN et al., 1992). In addition to these, eight
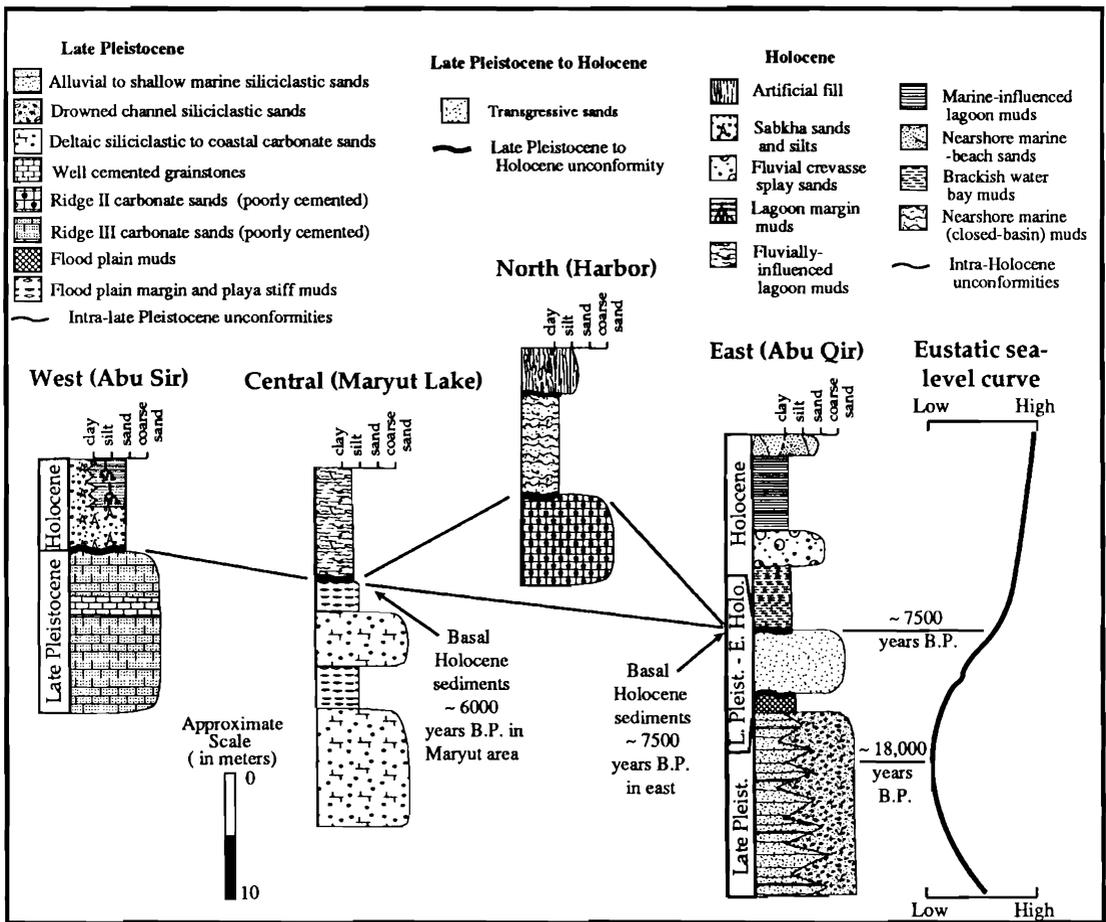
Figure 7. Generalized lithostratigraphic sections for four sectors in the study area. The various lithofacies, correlated largely on the basis of radiometric data, are related to sea-level changes during the late Pleistocene and Holocene. Generalized sea-level curve on right after Lighty *et al.* (1982) and Fairbanks (1989).

other facies and subfacies are recognized in the present study: late Pleistocene deltaic siliciclastic to coastal carbonate sands, carbonate-rich desert coastal sands, cemented limestones, distal flood plain stiff muds; and Holocene fluvially-influenced lagoon muds, lagoon margin muds, sabkha silts and sands, and nearshore marine (closed-basin) muds. The newly described facies are distinguished from previously defined Nile delta facies primarily by their higher proportion of carbonates.

## Late Pleistocene Sediment Types

Late Pleistocene core sections, radiocarbon dated at more than 12,500 years before present (BP), are composed primarily of sands with in-termittent stiff muds (Figure 7). In the eastern part of the study area this interval consists of tan to brown quartzose sands and green to brown stiff muds, whereas to the west, the late Pleistocene sequence consists of white to tan carbonate sands and yellow to green stiff muds (Figure 7). These regionally variable sand and stiff mud sequences represent several distinct environments of deposition along the western edge of the delta. Moreover, these late Pleistocene facies serve to define the boundary between the Nile delta to the east and the Western Desert coastal zone to the west.

### Alluvial to Shallow Marine Siliciclastic Sands

Yellowish brown (10YR 5/4) to light olive gray (5Y 5/2) to olive gray (10Y 5/2), very fine- to
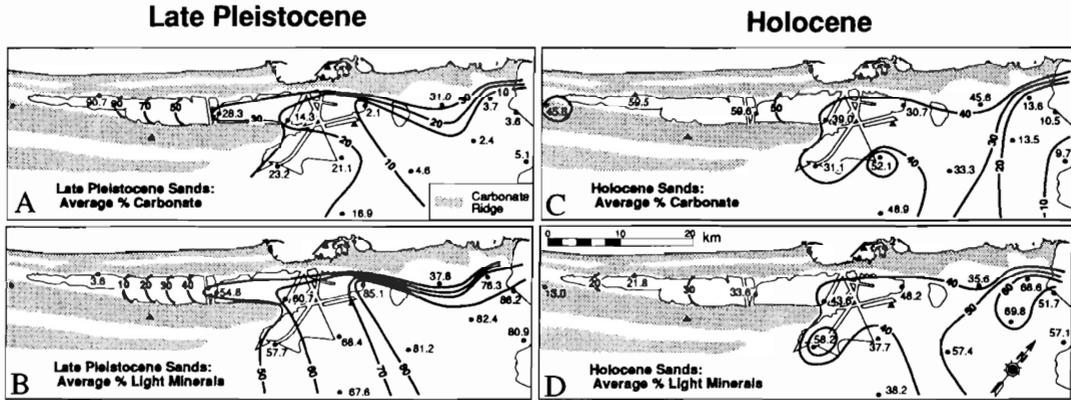
Figure 8. Isopleth map showing frequency distributions (averaged percent calculated from sand grain counts) of carbonate and light minerals for the sand size fraction in the late Pleistocene (A and B) and Holocene (C and D) sections. Westward increase in proportions of carbonate (and concurrent decrease in light minerals) for both the late Pleistocene and Holocene sections is the result of diminished influence of the River Nile to the west of Alexandria.

coarse-grained, rather poorly sorted sands are present in the lower portions of cores S-74 and S-78 in the eastern portion of the study area (Figure 7). These sands are primarily composed of iron-stained quartz; common accessory components include feldspar, mica, lithic fragments, heavy minerals and shell fragments. The proportion of carbonates (shells, shell fragments and unidentified carbonate particles) is generally low (Figure 8A). Fauna is rather sparse, although gastropods and ostracods, usually broken tests, are locally present. Core sections of this facies as long as 25 m have been recovered during Smithsonian drilling expeditions (MEDIBA, 1992); several well records reported by ATTIA (1954) indicate that this facies may locally exceed 50 m in thickness. The time of deposition of these sands cannot be accurately dated by the carbon-14 method: datable carbonate particles in the sands are, for the most part, reworked and originally formed well before actual burial. However, the stratigraphic position of these sands between, or below, dated stiff mud intervals indicates accumulation before 13,000 years BP. Composition of sands indicates they originated in the East African highlands, including the headwaters of both the Blue and White Nile (cf. SHUKRI, 1950; FOUCAULT and STANLEY, 1989; HAMROUSH and STANLEY, 1990). These sands are interpreted to be mostly alluvial deposits with intermittent shallow marine and lagoon components.

## Drowned Channel Sands

Light brown (5YR 5/6) to moderate yellowish brown (10YR 5/4), coarse- to very coarse-grained, poorly sorted, generally well rounded sands form a 29 m thick section in the lower portion of one core (S-73). Although the general composition of these sands is comparable to alluvial sands described above, they contain 30–50% very coarse, rounded and highly stained quartz grains, and 1–7% foraminifera. A radiocarbon date from the stiff mud interval at the top of these sands indicates that this facies was deposited before 12,000 years BP. The sphericity of the grains suggests that these sands were transported for a considerable distance, and their coarse-grained texture suggests that they were deposited in a major river channel. The presence of trace amounts of verdine/glauconite and foraminifera indicates that this paleochannel migrated over, reworked and redeposited former shallow marine and lagoon sediments. These sands are interpreted to have been deposited in the westernmost channel of the Late Pleistocene Nile alluvial system (cf. CHEN et al., 1992).

## Deltaic Siliciclastic to Coastal Carbonate Sands

Yellowish gray (5Y 8/1) to white (N9) to dark yellowish brown (10YR 4/2), fine- to coarse-grained, poorly sorted, carbonate-rich, lightly iron-stained sands are present in the lower portions of
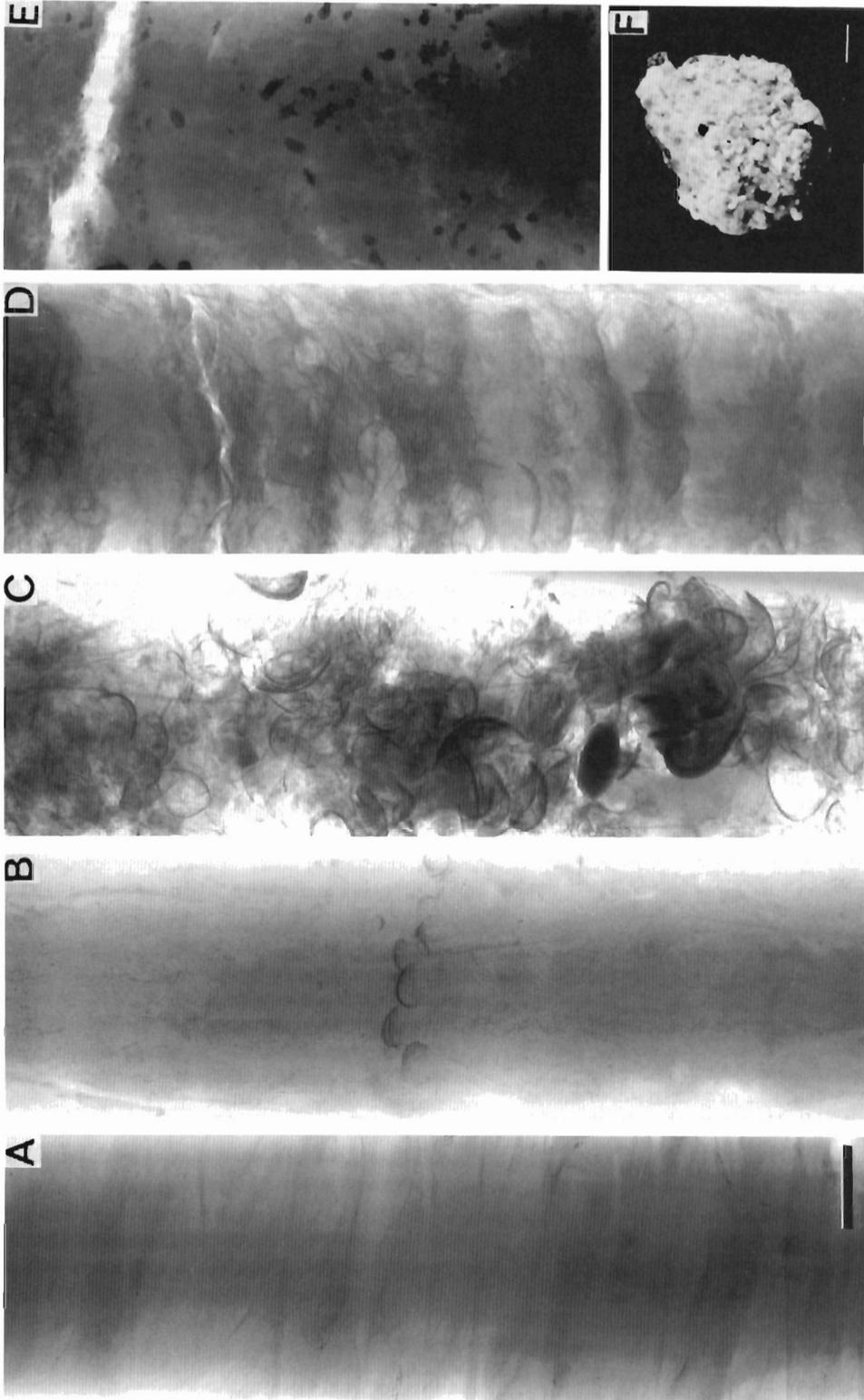
Figure 9. A–E, X-radiograph prints of representative facies from Smithsonian borings (bar = 2 cm). (A) alluvial cross-bedded sandy stiff mud of late Pleistocene age (core S-81, 10.5 m from core top). (B) brackish water bay mud of Holocene age, fairly homogenous, with layer of smaller valves, some concave-down (core S-77, 5.9 m). (C) lagoon coquina of Holocene age; randomly oriented articulated and individual pelecypod valves with minor mud matrix (core S-78, 4.8 m). (D) lagoon coquina of Holocene age; layered and preferentially oriented, articulated and individual pelecypod valves in mud (core S-79, 3.3 m). (E) lagoon margin mud of Holocene age with gypsum nodules (dark specks) and root traces (core S-84, 1.2 m). (F) carbonate aggregate of coarse sand size, formed of silt and fine sand-sized particles (broken shell, undifferentiated carbonate detritus and minor quartz) which are bound by carbonate cement (bar = 250 μm).

seven cores (S-77 to S-83) in the central study area (Figure 7). These sands are composed of variable mixes of quartz and carbonate, in which the proportion of carbonate increases westward (Figure 8A). The carbonate fraction, ranging from ~10 to 30% in this facies (Figure 8A), is composed of shells, unidentified carbonate particles and carbonate aggregates. Carbonate aggregates are herein defined to be mixtures of very fine sand- to silt-size broken shell, small undifferentiated carbonate detritus and minor quartz which are bound together by carbonate cement (Figure 9F). Gypsum is always present in considerable quantities (5–25%). Heavy minerals occur in significantly lower proportions than in the alluvial sands to the east. STANLEY and HAMZA (1992) reported small quantities of oolites from this interval. Although light iron-staining is common, these sands are less stained than the correlative alluvial sands to the east. Fauna, although generally sparse, is primarily composed of pelecypods, gastropods, foraminifera, calcareous algae and ostracods. Core sections as long as 34 m of this facies were recovered during Smithsonian drilling expeditions. The age of these sands can not be accurately dated by radiocarbon techniques, because datable carbonates in the sands were, for the most part, formed well before deposition and burial. However, the stratigraphic position of these sands between, or below, more reliably dated stiff mud intervals indicates a period of accumulation from ~16,500 to >39,000 years BP. We interpret these sands as having been deposited in a transitional sector between the Nile alluvial plain to the east and the Western Desert coastal plain to the west. The presence of quartz and heavy minerals (particularly in the east) indicates the influence of the River Nile (cf. HILMY, 1951); whereas high proportions of carbonate and gypsum (particularly in the west) are characteristic of desert coastal deposits (cf. EL SHAMI et al., 1971; GLENNIE, 1987). Detailed petrographic analysis of these sands indicates they are similar in composition to the easternmost portions of Ridges II and III (STANLEY and HAMZA, 1992).

### Desert Coastal Carbonate-rich Sands

Yellowish gray (5Y 8/1) to pinkish gray (5YR 8/1) to white (N9) rather poorly sorted, lightly cemented, medium- to coarse-grained, carbonate sands were recovered in the lower portions of one core (S-84). Carbonates compose 91% of this interval (Figure 8A) and consist largely of shell,

unidentifiable carbonate particles and carbonate aggregates. Accessory components include quartz and gypsum. Fauna is common, especially in the lower portion of the interval and includes pelecypods, foraminifera, gastropods and ostracods. Approximately 17 m of this facies was recovered in S-84; ATTIA (1954) reported >100 m of similar "marine sand" facies in well A-1 (Figure 1). Petrologic analysis indicates that these sands are characteristic of Ridge II or Ridge III deposits (STANLEY and HAMZA, 1992). Their age cannot be accurately determined by radiocarbon techniques. These sands are interpreted to be desert coastal deposits and record accumulation in nearshore, beach, sabkha and dune environments along a desert coast (cf. GLENNIE, 1987). Depositional conditions were similar to those presently encountered along the Egyptian Western Desert coast to the west of the study area (EL SHAMI et al., 1971). Based primarily on the proximity of S-84 to Ridge II, these carbonate-rich desert coastal sands are herein considered to be Ridge II sediments.

### Cemented Subsurface Carbonates

Yellowish gray (5Y 7/2) to very pale orange (10YR 8/2), well cemented limestones were recovered in borings S-84 and S-85 along the western extension (western sub-basin) of Maryut lake (Figure 7). The limestone units in the two borings are quite different and are thus described separately (detailed descriptions in STANLEY and HAMZA, 1992).

Yellowish gray (5Y 7/2) to medium light gray (N6), medium-grained, rather well sorted and well cemented grainstones occur in core S-84. STANLEY and HAMZA (1992) determined that this unit is composed of 87% fossils; however because these biogenetic components occur as well rounded, medium-grained allochems, they can only be recognized as fossils by microscope examination. STANLEY and HAMZA (1992) determined that this unit is composed of 39% algae and 25% foraminifera with minor amounts of gastropods and echinoids; ooids are a significant accessory component. The insoluble residue (quartz, etc.) of representative samples comprises <2% of the sands. This unit appears massive both in plain light and in x-radiographs. This interval is 1 m thick in core S-84. Radiocarbon analysis suggests that this unit is >40,000 years BP. STANLEY and HAMZA (1992) concluded that this grainstone unit was at least in part derived from eroded and reworked Ridge

III carbonates. Its well rounded, well sorted tex-
ture suggests significant reworking.

In contrast with the above, the limestone unit
in core S-85 is composed of very pale orange (10YR
8/2), medium- to very coarse-grained bioclastic
grainstones and algal boundstones. Large, well
preserved fossils are the principal component;
coated grains, ooids and unidentifiable fossil frag-
ments are important accessory components. Fau-
na in this unit include algae and foraminifera,
with lesser amounts of gastropods, echinoids and
ostracods. This unit is commonly laminated, cross-
bedded and contains many diastems. The stratum
is 4 m thick in core S-85. Radiocarbon analysis
suggests that this unit is >40,000 years old. This
limestone has a composition intermediate be-
tween those of Ridges II and III; however, the
high proportion of calcareous algae and presence
of characteristic amphistegin foraminifera indi-
cate a closer affinity with Ridge III (STANLEY and
HAMZA, 1992). The cross-bedded, coarse intervals
indicate deposition under high energy, subaque-
ous conditions. The high proportion of large, well
preserved fossils indicates short transport dis-
tances and relatively minor sediment reworking.

### Flood Plain Muds

Greenish gray (5GY 6/1) to dark yellowish brown
(10YR 4/2) sandy muds form the upper portion
of the late Pleistocene sequence in only one core
(S-73) in the eastern portion of the study area.
Sands occur as dispersed, matrix-supported grains,
or as discrete beds (to 14 cm thick) and lenses.
Irregularly shaped calcareous nodules (1 mm to
3 cm) are ubiquitous. Fauna and flora are sparse
to absent. In some sections, interbedded sands
and silts are current-ripple laminated. These sandy
muds are semi-consolidated and thus are termed
stiff muds. This facies is ~1.5 m thick in core
S-73. Radiocarbon dates from this facies indicate
an age >12,700 years BP. The sandy stiff muds
in core S-73 are interpreted to be channel over-
bank and crevasse-splay deposits which accu-
mulated in shallow ephemeral lakes and/or playas
in close proximity to distributary channels (cf.
BUTZER, 1976; ABU-ZEID and STANLEY, 1990; AB-
DEL WAHAB and STANLEY, 1991), under generally
arid conditions (cf. REINECK and SINGH, 1980;
COLLINSON, 1986; CHEN and STANLEY, in press).

### Flood Plain Margin and Playa Muds

Variegated, streaked and mottled stiff muds and
sandy muds occur in several cores (S-77 to S-83)

in the eastern portion of this study area (Figure
7). Some more common colors include: light olive
gray (5Y 5/2), dusky yellow (5Y 6/4), white (N9)
and grayish orange (10YR 7/4). These stiff muds
are primarily composed of quartz; accessory com-
ponents include carbonate, aggregate and gyp-
sum. Irregularly shaped calcareous nodules are
ubiquitous. Iron staining is common. Fauna and
flora are generally absent in the sand size fraction,
although there is one fossil-rich horizon in core
S-81. Cross-bedding is well developed in some sec-
tions (Figure 9A), whereas mud cracks are well
developed in others. These muds are semi-con-
solidated and thus are termed stiff muds. This
facies ranges in thickness from 0.5 to 8.8 m. One
to three separate stiff mud intervals may occur in
the cores (Figure 7). Radiocarbon data indicate
that these stiff muds range in age from ~16,500
to >38,000 years BP.

Previous investigations in the north-central Nile
delta (ARBOUILLE and STANLEY, 1991; STANLEY et
al., 1992) recognized two distinct stiff mud types:
overbank and interdistributary lagoon facies.
Compared to these two facies, the playa stiff muds
are more green, yellow and white (as opposed to
brown), generally have a higher carbonate con-
tent, are more oxidized, and contain almost no
plant matter. Cross-bedded sandy muds up to 20
cm thick (Figure 9A) indicate subaqueous depo-
sition, whereas well-developed caliche horizons
and mudcracks indicate subaerial exposure. A
general absence of vegetation is recorded by lack
of both root traces and plant material. The stiff
muds of the study area are interpreted to have
been deposited in ephemeral lakes and playas near
the edge of the Nile delta flood plain under gen-
erally arid conditions (cf. GUSTAVSON, 1991).

### Late Pleistocene to Early Holocene Transgressive Sands

Olive gray (5Y 3/2) to yellowish brown (10YR
4/2), fine- to coarse-grained, rather poorly sorted
sands occur in the lower portions of cores S-72,
S-75 and S-76 in the eastern study area (Figure
7). These sands are primarily composed of un-
stained quartz; common accessory components
include heavy minerals, shell fragments and ver-
dine/glauconite. Undifferentiated carbonate and
shell fragments comprise as much as 35% of the
sand fraction. Fauna, although generally sparse,
includes gastropods, pelecypods, ostracods and
foraminifera. This facies ranges to 10 m thick in
study area cores. The sands per se have not been

dated, but radiocarbon dates from Holocene muds immediately above these sands indicate they were deposited before 7,500 years BP.

Several Nile delta studies to the east (e.g., COUTELLIER and STANLEY, 1987; ARBOUILLE and STANLEY, 1991; STANLEY et al., 1992; CHEN et al., 1992) have interpreted this facies to be marine transgressive sands which were deposited during the last rapid rise in sea level (Flandrian transgression). This facies is the product of reworking of late Pleistocene alluvial and shallow marine deposits which resulted in concentration of sands. Carbonate content in this facies increases westward (STANLEY and HAMZA, 1992): increased proportions of marine carbonates relative to terrestrial siliciclastics is a function of the decreased influence of the River Nile system at and west of the Alexandria region.

### Holocene Sediment Types

Nile delta sediments of Holocene age began to accumulate ~7,500 years BP in the eastern part of the study area as the rate of sea-level rise began to decrease (cf. MÖRNER, 1976; cf. LIGHTY et al., 1982; cf. FAIRBANKS, 1989; STANLEY, 1990; see eustatic sea-level curve in Figure 7). Unlike the northeastern Nile delta (COUTELLIER and STANLEY, 1987; STANLEY et al., 1992) there are no open marine (prodelta, delta-front) facies of Holocene age in the present study area. In addition, unlike Holocene sequences to the east, which are composed of several distinct facies (CHEN et al., 1992), Holocene sequences in the central and western sectors of the study area are composed of only one facies.

An unconformity separates the Holocene from underlying alluvial or coastal sands (BERNASCONI et al., 1991; STANLEY et al., 1992). In the present study area, lag deposits comprising shells, coarse sands, and rounded carbonate pebbles occur at or just above this hiatus in many cores. Radiocarbon dates indicate that this lacuna is larger in the southern and western part of the study area.

### Brackish Water Bay Muds

Olive gray (5Y 3/2), grayish black (N2), to greenish black (5 GY 2/1) soft, homogenous muds occur near the base of the Holocene sequence in five cores (S-72 to S-76) to the south of Abu Qir (Figures 1, 7). Common sand-size components include light and heavy minerals, micas and shells. The muds are generally fossiliferous, with bi-

valves, gastropods and foraminifera as the most common taxa. Shells in brackish water bay facies tend to be smaller (0.5–2.0 mm) than those in lagoons, and are usually more dispersed (Figure 9B). Horizontal and uneven laminae are commonly observed in muds; stratification, in some cases, is highlighted by concentrations of fossils (Figure 9B). Brackish water bay mud sections range in thickness from 1.2 to 7.0 m. Radiocarbon dates indicate that this facies was deposited primarily between 7,000 and 5,000 years BP.

Carbonate pebbles commonly occur in brackish water bay muds and are composed of irregularly shaped calcareous siltstone and grainstone. Thin-section analysis shows that these pebbles were derived from the adjacent Abu Sir Ridge II (cf. EL FAYOUMY et al., 1975; STANLEY and HAMZA, 1992; CHEN et al., 1992). The pebbles were probably washed from the ridge and incorporated in bay deposits during storms.

Molluscan assemblages from bay facies indicate brackish water conditions with significant marine influence. These faunas also suggest accumulation at water depths ranging from 5 to 7 m (M. P. BERNASCONI, written communications, 1991, 1992). Combined petrologic and molluscan community analyses indicate that these muds accumulated in generally brackish water, but in deeper, more marine-influenced conditions than those of lagoons.

### Nearshore Marine (Closed-basin) Muds

Gray, sandy and silty muds were described in numerous engineering cores (E-2 and E-3 are examples) from the harbor area of Alexandria (Figures 1, 7). The muds are characteristically organic-rich, shelly and have a hydrogen sulfide odor. Root traces are common. This mud interval ranges from 6 to 11 m thick. The age of the base of the muds above carbonate sands has not been radiocarbon-dated, but most probably is of mid-Holocene age. Organic-rich muds are currently being deposited in the semiclosed Eastern and Western harbors of Alexandria, from depths of several meters close to shore to a maximum of 8 m. Recent and sub-recent sediment is anthropogenic (municipal and industrial waste) and is highly polluted (EL-SAYED et al., 1988; DOWIDAR and ABOUL KASSIM, 1986).

### Holocene Lagoon Facies

Previous studies described older Holocene and modern lagoon mud facies in the northern Nile

delta to the east (ARBOUILLE and STANLEY, 1991; LOIZEAU and STANLEY, in press). Based on detailed petrological and molluscan community analyses, three mud subfacies are distinguished in the northwest Nile delta region: marine-influenced lagoon, fluvially-influenced lagoon, and lagoon margin.

**Marine-influenced Lagoon Muds.** Olive gray (5Y 3/2) to dark gray (N3) plant-rich muds and silts occur in the eastern part of the study area (S-72 to S-78). The sand fraction is primarily composed of quartz and shell; accessory components include heavy minerals, mica and plant debris. Some intervals consist almost entirely of molluscs (Figure 9C). Biogenic components include characteristic ostracods (PUGLIESE and STANLEY, 1991), benthic foraminifera (EL-WAKEEL *et al.*, 1970; KULYK, 1987), molluscs (BERNASCONI *et al.*, 1991), sponge spicules and diatoms; plant matter is common to abundant. Bedding may be undisturbed or completely obscured by bioturbation. Where undisturbed, bedding features include: horizontal and wavy lamination, small-scale ripple cross lamination, and lenticular to flaser bedding (CHEN *et al.*, 1992, their Figure 5B; STANLEY *et al.*, 1992, their Figure 3). The thickness of this lagoon subfacies ranges from 1 to 9 m. Radiocarbon data indicate that lagoon deposits accumulated from ~5,000 years BP to the present. Molluscan paleocommunity analysis on two cores (M. P. BERNASCONI, *written communications*, 1991, 1992) indicates that these muds were deposited in a marine-influenced lagoon which was directly connected to the sea, and supplied with fresh water by Nile distributaries. These deposits are directly comparable with those accumulating in the modern Idku lagoon (LOIZEAU and STANLEY, in press), and with adjacent Holocene lagoon mud facies described by COUTELLIER and STANLEY (1987), ARBOUILLE and STANLEY (1991), STANLEY *et al.* (1992), and CHEN *et al.* (1992).

**Fluvially-influenced Lagoon Muds.** Olive gray (5Y 3/2) to dark gray (N3) to greenish gray (5GY 6/1) muds and silts occur in the central and western part of the study area (S-77 to S-84). The sand fraction in these muds is primarily composed of quartz and shell; accessory components include unidentified carbonate particles and gypsum. Many intervals consist almost entirely of molluscs (*cf.* Figure 9C). In contrast to the marine-influenced lagoon subfacies, the freshwater influenced lagoon subfacies has lower proportions of heavy minerals, mica, verdine/glauconite and forami-

nifera, and higher proportions of gypsum and carbonates (Figures 8, 10). Fauna is dominated by pelecypods, particularly *Cardium*; other fauna include gastropods, ostracods, and foraminifera. Bedding is generally obscured by bioturbation and shell; however, in places, shells form distinct layers (Figure 9D). The thickness of this lagoon subfacies ranges from 2 to 9 m. Radiocarbon data and historical records indicate that these fluvially-influenced deposits accumulated from ~6,100 to 700 years BP. Molluscan community analysis suggests that the mud and shell sequence was deposited in brackish water with significant freshwater influence (M.P. BERNASCONI, *written communication*, 1992). This subfacies is interpreted to have been deposited in a basin which was not directly connected to the sea, and was fed directly by one or more perennial River Nile channels.

Gypsum in this facies (Figure 10F) is interpreted to have formed postdepositionally, probably between the twelfth and nineteenth centuries. During this period, all Nile delta channels which had supplied fresh water to Lake Mareotis had silted up so that the lake level fell, and this region became a salt lake and sabkha. Under these evaporitic conditions, saline groundwater precipitated gypsum in the buried freshwater lake deposits. It is of note that gypsum is currently forming beneath the surface of the nearby El Dekheila-Abu Sir and Mallahet Maryut depressions (WEST *et al.*, 1979; ALI and WEST, 1983).

**Lagoon Margin Muds.** Light olive gray (5Y 6/1) to yellowish gray (5Y 7/2) muds occur primarily in core S-84, in the western extension of Maryut lake (Figures 1, 7). The sand fraction in these muds is primarily composed of weathered limestone (Ridge II) residuum, carbonate aggregates and quartz. Significant accessory components include plant material, gypsum and shell (Figure 10). Limestone pebbles (to 10 cm) occur locally. Fossils are generally sparse; however, there is one fossil-rich horizon in which foraminifera are especially abundant. The unit has been thoroughly bioturbated by roots. Discrete quartz sand layers are generally absent. Gypsum nodules are commonly noted in x-radiographs (Figure 9E). This facies is 2 m thick in S-84. No radiocarbon dates are available for this unit. In contrast to marine-influenced and freshwater-influenced lagoon sediments, this subfacies by being lighter colored (more oxidized), contains higher proportions of gypsum, roots and root traces, and lower proportions of shell. The gypsiferous mud, abundant root traces
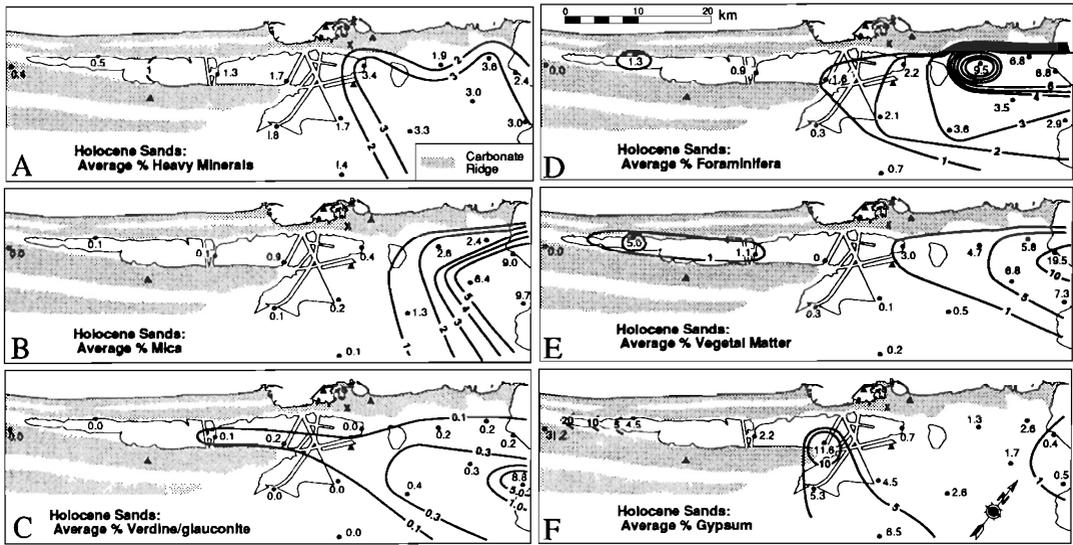
Figure 10. Isopleth map showing frequency distributions (averaged percent) of selected sand-size components for the Holocene section. Distributions are discussed in text.

and its proximity to Ridge III indicate that these deposits accumulated along a lagoon margin.

### Holocene Sand Facies

Four sand facies of Holocene age are recognized in the study area: nearshore marine-beach, lagoon, fluvial channel to crevasse-splay, sabkha and alluvial fan. Each of these sand facies is described below.

**Nearshore Marine to Beach Sands.** Yellowish gray (5Y 7/2 to 5Y 8/1) mostly fine- to medium-grained sands occur in the upper portions of one core (S-73). These sands are characterized by relatively low proportions of lightly iron-stained quartz, and high proportions of heavy minerals. Verdine/glauconite is a common accessory component. Shells are sparse and occur mostly as fragments. This facies is 1.5 m thick in core S-73. Radiocarbon dates indicate that these sands were deposited within the past 3,400 years. Low proportions of stained quartz and high proportions of heavy minerals are characteristic of sands extensively reworked in a swash zone where denser grains are concentrated (STANLEY et al., 1992). Verdine/glauconite indicates that these sands accumulated in or near a shallow marine environment (cf. PIMMEL and STANLEY, 1989).

**Lagoon Sands.** Pale yellowish brown (10YR 6/2) to yellowish gray (5Y 7/2), very fine- to fine-grained, moderately to well sorted sands occur as beds and lenses within lagoon mud facies in cores S-72, S-73, S-75, S-76 and S-78. Quartz is the primary constituent and mica is common to abundant; other accessory components include shell fragments, verdine/glauconite, pyrite and gypsum. Sand layers within muddy lagoon facies range from a few millimeters to 9 cm thick. Based primarily upon petrology, ARBOUILLE and STANLEY (1991) distinguished two lagoon sand subfacies: fluvially-influenced and storm wash-over. Of the two, storm wash-over sands contain relatively higher proportions of fossils and verdine/glauconite, whereas fluvially-influenced lagoon sands contain relatively higher proportions of plant debris. Lagoon sands of the present study are primarily fluvially-influenced.

**Fluvial Channel to Crevasse-splay Sands.** Olive gray (5Y 3/2) to grayish olive (10Y 4/2), generally fine-grained, moderately to poorly sorted sands occur in cores S-73 and S-75 (CHEN et al., 1992). Quartz is the main constituent; accessory components include heavy minerals, mica and gypsum. The few fossils present, such as in core S-73, are broken and abraded. The thickness of this facies in the study area ranges from 1 to 4 m. Radiocarbon data indicate that these sands were

deposited as early as 5,900 years BP (S-75) and as late as 2,900 years BP (S-73). The high proportion of iron-stained quartz and absence of nonreworked fossils indicate that these sands were deposited in river channel and adjacent crevasse-splay environments (cf. STANLEY and CHEN, 1991; CHEN et al., 1992). These Holocene sands are readily distinguished from the late Pleistocene alluvial sands: the Holocene fluvial sands are primarily composed of fine-grained, lightly iron-stained quartz, whereas the late Pleistocene alluvial sands are primarily composed of coarse-grained, well rounded, highly iron-stained quartz.

Sabkha to Alluvial Fan Silty Sands. Very pale orange (10YR 8/2) to grayish orange (10YR 7/4), very fine-grained sands and silts are best developed in core S-85. The sands and silts are primarily composed of carbonate with gypsum; accessory components include quartz and shell fragments. Carbonates are most commonly composed of weathered limestone fragments and carbonate aggregates. Fauna is very sparse. This subfacies is 6 m thick in S-85. Because of reworking, these sands cannot be accurately dated by the radiocarbon method. The high proportion of weathered limestone and the proximity of core S-85 to Ridge III indicate these are alluvial fan deposits: in addition, the high proportion of gypsum and silt suggest these are sabkha sediments. It is of note that core S-85 was recovered in the Mallahet Maryut depression; ALI and WEST (1983) described the upper 1 m of sediments in this depression as sabkha deposits.

## FACIES AS RELATED TO SEA LEVEL, NEOTECTONISM AND CLIMATE

Petrologic analyses described above highlight the diversity of late Quaternary coastal and terrestrial sediment types in the Alexandria region. A summary of the laterally variable lithofacies sequences is represented by generalized sedimentary sequences from four sectors of the study area (Figure 7). In the following sections, an attempt is made to place these late Quaternary lithofacies sequences in a comprehensive stratigraphic and paleogeographic context. To do so requires that each facies be related to principal factors which determine sediment distribution. Here, lithofacies distributions in time and space are considered in terms of sea level, tectonism and climate. A fourth major factor, sediment transport processes, is considered in later sections.

### Sea-level Factor

Late Quaternary lithofacies in the Nile delta study area were deposited during the most recent eustatic sea-level cycle: from the last Pleistocene highstand (~35,000 to 30,000 years BP), to the last Pleistocene lowstand (~20,000 to 18,000 years BP), to the present highstand (cf. eustatic curves of LIGHTY et al., 1982; FAIRBANKS, 1989; see also PIRAZZOLI, 1992). Tide-gauge data for the past 50 years from the Alexandria region indicate that relative sea level has continued to rise and could be as much as 1.8 to 2.5 m above its present level by 2100 (EL-FISHAWI and FANOS, 1989; FRIHY, 1992).

To better understand the influence of sea level oscillations on coastal development, impacts of late Pleistocene to Holocene sea-level changes on subsurface lithofacies distributions are discussed.

(1) Late Pleistocene carbonate ridges record sea-level stands that are generally higher than at present (SHUKRI et al., 1956; BUTZER, 1960). Some workers have proposed that these ridges originated as submarine coastal bars which record sea level at the time of their formation (ZEUNER, 1952; SHUKRI et al., 1956); other workers, however, realized that significant portions of these ridges are of coastal dune origin and thus do not reflect sea level at the time of deposition (BUTZER, 1960). Recent work has shown that several minor sea-level cycles are recorded within a single ridge (HASSOUBA, 1980; HASSAN et al., 1986).

(2) Younger late Pleistocene siliciclastic alluvial to shallow marine sand, local drowned valley sand, flood plain stiff mud, deltaic siliciclastic to coastal carbonate sand, and carbonate coastal sand accumulated from earlier than ~30,000 to 11,000 years BP. Thus, they were deposited during the last Pleistocene sea-level highstand, last major eustatic lowering, and early phases of the subsequent very rapid sea-level rise. The coastline at that time was generally northward (seaward) of its present position, having migrated as much as 50 km to the north of the present coast, just landward of the present-day shelfbreak (SUMMERHAYES et al., 1978; MALDONADO and STANLEY, 1979; ABDEL WAHAB and STANLEY, 1991).

(3) Marine transgressive sands accumulated in the eastern part of the study area from 11,000 to 8,000 years BP as sea level continued to rise. This late Pleistocene to early Holocene rapid rise caused the coastline to retrograde southward of the present-day Nile delta shoreline to the east of Abu

Qir. An unconformity developed at the base of transgressive sands as the shoreline migrated southward (landward) and marine currents and waves reworked late Pleistocene sediments.

(4) An unconformity also occurs at the base of the Holocene sequence throughout the study area. Radiocarbon dates indicate that this lacuna is variable in duration and that Holocene sedimentation commenced ~7,500 to 5,000 years BP. In particular, this surface of erosion and (or) non-deposition continued well into the mid-Holocene in the southern and western portion of the study area (Figure 7).

(5) By ~7,500 years BP the rate of sea-level rise decelerated such that the rate of sediment input began to predominate over the rate of sea-level rise; consequently, aggradation and progradation of Nile delta sediments began to accumulate on the unconformity.

(6) Brackish water bay muds were deposited in the eastern sector of the study area from ~7,500 to 5,000 years BP, while the southern and western sectors of the study area remained emergent.

(7) By ~5,000 years BP, as sea level continued to rise, the central and western sectors of the study area were inundated and fluvially- to marine-influenced lagoon conditions were established.

(8) From ~5,000–1,000 years BP, as sea level has continued to slowly rise, marine-influenced lagoon muds and fluvial sands accumulated in the eastern sector and fluvially-influenced lagoon, lagoon margin and sabkha sediments accumulated in the western sector of the study area. During this period, sea level rose from about −5 m to −1 m (cf. LIGHTY et al., 1982).

Tectonic Factor

Lithofacies distributions can be affected by displacement of land surface (subsidence or emergence) relative to sea level in a similar way as they can by a change in sea level relative to land surface. It is thus imperative in paleogeographic reconstructions to distinguish the effects of these two factors: eustacy and tectonism. The late Quaternary sea-level history, as discussed in the previous section, is reasonably established. Here, evidence for tectonism in the Alexandria region and its possible effects on lithofacies distributions are discussed.

Several studies have found archeological and geological evidence which indicate late Quaternary tectonic activity in the study area. Obser-

vations on submerged Greek and Roman ruins in the Alexandria and Abu Qir regions lead JONDET (1916), TOUSSOUN (1934), MORCOS (1985) and EL-SAYED (1988b) to conclude that ruins as old as 2,500 years along the coast had submerged 2 to 5.5 m. Several observations suggest that neotectonics and seismicity may have been a factor. For example, four major earthquakes which shook Alexandria in the fourth century A.D. (DE COSSON, 1935) are nearly coincident with a major tectonic event in the eastern Mediterranean during the fifth century AD; this event likely resulted in vertical displacements at numerous localities around the Mediterranean basin (PIRAZZOLI, 1987). There is, in fact, considerable evidence of fault displacement in the study area. BUTZER (1960) pointed out that several of the late Pleistocene carbonate ridges terminate at the same longitude; he attributes this to possible displacement along north-south oriented faults (Figure 2, inset). From geophysical surveys, SHATA (1955) and EL RAMLY (1968, 1971) described subsurface folds in the region. EL RAMLY (1971) proposed that the carbonate ridges were delimited by successive earth movements. From satellite images, EL SHAZLY et al. (1975) described an important system extending northwestward from Wadi Natrun toward the Borg el Arab region. HASSOUBA (1980) attributed the eastward disappearance of late Pleistocene carbonate ridges to increased isostatic loading, and perhaps faulting, to the east under the weight of thick River Nile sediments. Based primarily on satellite imagery, NEEV et al. (1982, 1985, 1987) suggested that the Alexandria region lies within a major northeast-southwest oriented fracture zone (a left-lateral megashear) that extends from the Israel-Lebanon coast southwestward through central Africa. In this scheme, the Alexandria region is located along the northeast-southwest oriented Qattara-Eratosthenes shear (NEEV et al., 1982). These authors recognized three sets of photolineaments in the Alexandria region: NE-SW, WNW-ESE and E-W. It has been proposed that late Pleistocene carbonate (kurkar) ridges in the study area are tectonically elevated and formed along pre-existing lineaments (NEEV et al., 1987).

An isopachous map of the total Holocene section, based on analysis of Smithsonian and engineering borings, is useful in differentiating the tectonic from sea-level factor. It is of note that field penetrometer measurements of Holocene sediment strength in cores show little variability both vertically and laterally. It hence appears that
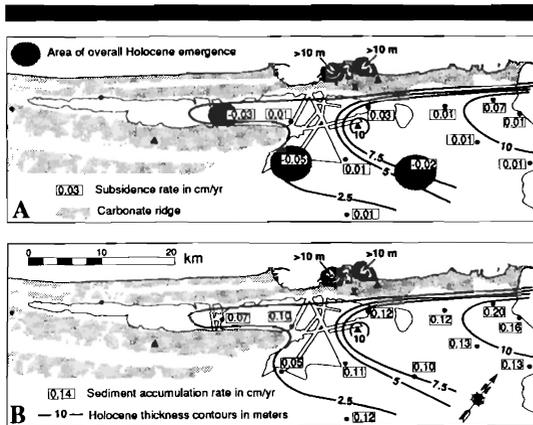
Figure 11. Isopachous maps of the total Holocene thickness (contours in meters). (A) map depicting long-termed averaged Holocene subsidence-emergence rates in cm/yr. Areas with overall emergence are denoted by negative numbers. (B) map showing long-term averaged Holocene sediment accumulation rates in cm/yr.

sediment compaction has not significantly modified lithofacies thickness trends.

Figure 11 shows that Holocene sediments thicken markedly to the east, towards Abu Qir bay. The most notable exception to this overall thickness trend is in the harbor area of Alexandria where isolated pods of Holocene sediments attain thicknesses of more than 10 m. It should be kept in mind, however, that availability of Holocene thickness data for the region is unevenly distributed. For example, no thickness data currently exist for El Dekheila-Abu Sir depression I, or for the nearshore, open marine shelf, north of the Abu Sir-Alexandria coast.

Long-term land displacement (subsidence or emergence) rates have been calculated for all cores in the study area (cf. method of STANLEY, 1988). To obtain conservative values, calculations for each core involve: (1) determining the age and depth of the lowest-oldest radiocarbon-dated Holocene sample for each core; (2) estimating the sea-level position, relative to the present stand, at the time indicated by the dated sample, using a eustatic curve (cf. LIGHTY et al., 1982); (3) subtracting the total Holocene thickness for that core from the depth of sea level projected from eustatic curves at that time: this subtraction is done to account for accommodation space (WILGUS et al., 1988) made available by subsequent sea level rise; and (4) division of the remaining sediment thickness (or accommodation space made available by sub-

sidence) by the radiocarbon age of that core sample. Using core S-77 as an example, the lowest radiocarbon-dated sample has an age of 6,170 years BP at a depth of 8.7 m. Eustatic sea-level curves indicate that, at 6,170 years BP, sea level was 7 m below its present stand, and thus the thickness of Holocene sediment, which can be attributed to vertical land motion, is $8.7 - 7 = 1.7$ m. A lowering rate of 0.03 cm/yr (30 cm/100 yrs) is calculated by dividing 1,700 cm (1.7 m) by 6,170 years. Given a maximum one standard deviation error of 140 years (as reported by Beta Analytic), the subsidence rates are accurate to within 5%. Error introduced by inaccuracies in the estimated sea level rise, however, is not known.

The above calculations assume that present ground elevation of the boring site is at sea level, and that the radiocarbon-dated layer was deposited at sea level. However, surface elevations from which some of the borings in this region were taken are actually below sea level (Figure 4). Thus, long-term subsidence rates calculated for the study area are minimal. Calculations that result in negative values, at 3 of the 14 Smithsonian core sites in the western and southwestern sectors, indicate minor emergence during the Holocene.

Calculated long-term vertical land displacement rates indicate minor subsidence (to 0.07 cm/yr) in the east (Figure 11A) and minor emergence (to −0.5 cm/yr) in the west. Low subsidence values are a marked contrast to regions just to the east and northeast where subsidence rates as high as 0.45 cm/yr are recorded in the Rosetta promontory region (CHEN et al., 1992). Emergence, at least locally, would help explain the presence of one or more hiatuses within various Holocene sections. Radiocarbon dates from study area cores demonstrate that the most significant hiatus occurs at the base of the Holocene, and that this lacuna is greatest in the southwest.

Ruins of the ancient Hellenistic city of Canopus in Abu Qir bay (Figure 3; TOUSSOUN, 1934) now lie as much as 5 m below sea level. Tousson (1934) assumed that these Hellenistic (~500 BC and younger) ruins were originally as much as 3 m above sea level, which would imply that they have been submerged as much as 8 m during the past 2,500 years. According to many eustatic curves (cf. LIGHTY et al., 1982; FAIRBANKS, 1989), sea level has risen ~2.5 m during the past 2,500 years. From this, it has been suggested that the ruins of Canopus may have tectonically subsided at a rate of 0.22 cm/year (CHEN et al., 1992), which is sig-

nificantly higher than rates to the south and west (Figure 11A). Subsidence at Canopus approaches rates recorded in the Rosetta promontory to the east. From observations on the depths of Hellenistic and Roman ruins in the Alexandria harbor region (JONDET, 1916; MORCOS, 1985; EL-SAYED, 1988b), it may be concluded that the Alexandria coast (Figure 3) has been submerged at rates of 1 to 2 m/1,000 yr. El Sayed (1988b) concluded that the tectonic factor is an important component of this submergence. From our present study, we interpret the tide-gauge data for Alexandria, cited earlier (increased water level of 0.18 to 0.25 cm/year), as recording both eustatic sea level rise (to 0.1 cm/year) and tectonic land subsidence (to ~0.15 cm/year).

From the above considerations, it is apparent that the petrologically variable Holocene facies in the study area accumulated in a sector of the delta which has undergone modest vertical land displacement when compared to areas to the east (ARBOUILLE and STANLEY, 1987; CHEN et al., 1992). The modest rates would explain the absence of open marine facies (prodelta and delta-front) in the Alexandria region (Figure 7).

### Climatic Factor

Climatic change can affect sea-level fluctuations, coastal processes, river channel migrations, and therefore, sediment distribution. Thus, in order to more fully define late Quaternary paleogeography in the Alexandria region, it is important to differentiate the role of climate from the other controlling factors. The late Quaternary climatic history of the eastern Sahara and Nile valley region (ADAMSON et al., 1980; PAULISSEN and VERMEERSCH, 1989; PETIT-MAIRE, 1989) during the past 35,000 years can be summarized as follows: from ~35,000 to 25,000 years BP climate was arid; from ~25,000 to 20,000 years BP conditions were somewhat more humid; from ~20,000 to 12,500 years BP climate was generally cool and dry; from ~12,500 to 5,000 years BP climate was more humid resulting in high floods; and from ~5,000 years to the present, climate has been arid. Archeologic evidence indicates that the climate in the Alexandria region has become significantly drier during the past 2,000 years (DE COSSON, 1935).

Several late Pleistocene lithofacies, and their distribution, can be related to syndepositional climatic conditions. In the western part of the study area, medium to coarse carbonate-rich sands of late Pleistocene age are characteristic of desert coast deposits (cf. EL SHAMI et al., 1971; GLENNIE, 1987). In the eastern part of the study area, medium to coarse, poorly sorted, iron-stained sands of late Pleistocene age (particularly those which accumulated between ~20,000 and 12,500 years BP) were deposited under arid conditions by a seasonally dry, braided river system (cf. ADAMSON et al., 1980; STANLEY et al., 1992). Flood-plain and playa stiff muds of late Pleistocene age accumulated locally in ephemeral interchannel depressions; calcareous nodules and gypsum in these flood-plain muds suggest repeated seasonal wetting and drying in an arid to semiarid climate (cf. GUSTAVSON, 1991; CHEN and STANLEY, in press).

Climate has also been a major factor in determining sediment type and distribution during Holocene times (~7,500 years BP to the present). Reduced proportions of coarse, iron-stained sands in Holocene river channel deposits indicate more humid conditions. Moreover, the transition from thick late Pleistocene alluvial sands to discrete Holocene fluvial lithosomes in mud (Figure 7) record a change from a seasonally dry, braided river in the late Pleistocene to a perennial, meandering river system in the Holocene. Fluvially-influenced lagoon deposits in the western part of the study area also record the presence of a perennial river system. In contrast, gypsiferous sabkha deposits in the western part of the study area (WEST et al., 1979; ALI and WEST, 1983) indicate that, overall, the Holocene climate has remained arid.

The above climatic observations concur with those made in the delta regions to the east (ARBOUILLE and STANLEY, 1991; STANLEY et al., 1992; CHEN et al., 1992). In our view, climate has significantly influenced sediment composition and facies distribution in the Nile delta study area, but to a lesser extent than either eustatic sea-level or tectonic oscillations. For example, the overall transition from late Pleistocene alluvial to Holocene coastal deposition records the change from a major sea-level lowstand to a highstand. Moreover, variable Holocene sediment thicknesses and lithofacies sequences record variable subsidence histories across the study area (Figure 7).

### RATES OF SEDIMENT ACCUMULATION

Holocene sediment accumulation rates (Figure 11B) are calculated to more accurately interpret facies distribution in time and space and, more specifically, to better differentiate the effects of sea level and tectonism on lithofacies distribution.
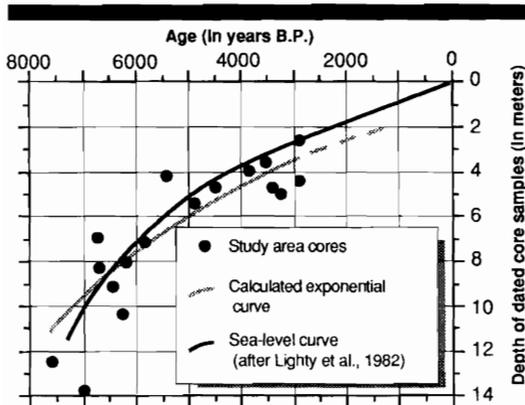
Figure 12. Graph showing core depth versus radiometric age for 17 samples from 11 cores. The exponential curve was calculated from these data. Superimposed on the calculated curve is a generalized eustatic sea-level curve (from Lighty *et al.*, 1982); depth is in meters below sea level. The near-coincident calculated and eustatic curves implies (1) Holocene sedimentation rates are largely controlled by rate of sea-level rise, and (2) tectonic subsidence was minor during the Holocene. See text for discussion. Error in radiocarbon dates, as reported by Beta Analytic Inc., represent one standard deviation and range from ±60 to ±140 years.

Accumulation rates have been calculated in two ways, as described below.

Long-term averaged rates of sediment accumulation were calculated for each of the fourteen Smithsonian core sections. Calculations first involved determination of core depth and age of the oldest radiocarbon-dated Holocene sample in each core. Averaged accumulation rates are calculated by dividing the depth of each sample by its age in all cores. Estimated values take into account possible errors associated with the radiocarbon date.

Holocene sediment accumulation rates across the study area (Figure 11B) generally decrease from northeast (0.20 cm/yr, or 200 cm/1,000 yrs) to southwest (0.02 cm/yr, or 20 cm/1,000 yrs): these values are significantly lower than rates in the Nile delta to the east (COUTELLIER and STANLEY, 1987; ARBOUILLE and STANLEY, 1991; STANLEY *et al.*, 1992; CHEN *et al.*, 1992).

Changes in sediment accumulation rates over time were determined, using 17 radiocarbon-dated samples of Holocene age from 11 cores. A graph showing depths of dated samples versus age of these samples (Figure 12) reveals a marked decrease in accumulation rates from ~7,500 to 5,000 years BP, and then a more gradual decrease in

rates from ~5,000 to 3,000 years BP. These trends are highlighted by a calculated exponential curve. The dispersal of data points may, in part, reflect irregular, pre-Holocene topography on which sediments were deposited.

The calculated accumulation curve is nearly co-incident with (~0.5 m below) the general eustatic sea-level curve of LIGHTY *et al.* (1982). This parallel trend of the accumulation and sea-level curves indicates that major changes in Holocene accumulation rates are primarily controlled by changes in rates of sea-level rise. This would support our contention that Holocene eustatic sea-level fluctuations are the principal influence on sedimentation in the region.

An average regional sediment accumulation rate of 0.10 cm/yr for the past 5,000 years is estimated from the overall slope of the calculated curve in Figure 12. This calculated rate is the same as the rate of sea-level rise. These comparable rates demonstrate that, overall, subsidence in the study area during the Holocene was modest to negligible.

## REGIONAL LITHOFACIES CORRELATION AND GEOMETRY

Integration of all pertinent petrologic, faunal and radiometric data for each study area core, and subsequent core-to-core correlations define late Quaternary lithofacies distributions in time and space. Correlations and lithofacies analysis take into account the relative impact of sea level, tectonism and climate on sedimentation. In addition, the effects of sediment transport processes on lithofacies distributions need also to be considered here. Salient features of lithofacies distributions are summarized in Figures 13 and 14, and are described below, from oldest to youngest.

(1) Petrographic data show that Ridges I, II and III are lithologically distinct (STANLEY and HAMZA, 1992), and paleontologic data indicate these ridges were deposited during separate time periods (SHUKRI *et al.*, 1956). Each ridge is interpreted to be composed of nearshore marine to coastal dune sediments which accumulated during an overall sea-level highstand. These ridges contain interbedded paleosols, caliche horizons and marine deposits which record minor sea-level fluctuations during ridge development (*cf.* HASSAN *et al.*, 1986; STANLEY and HAMZA, 1992). Ridge II and Ridge III carbonates are interpreted to be separated by an unconformity (see also SHUKRI *et al.*, 1956, their Figure 2).
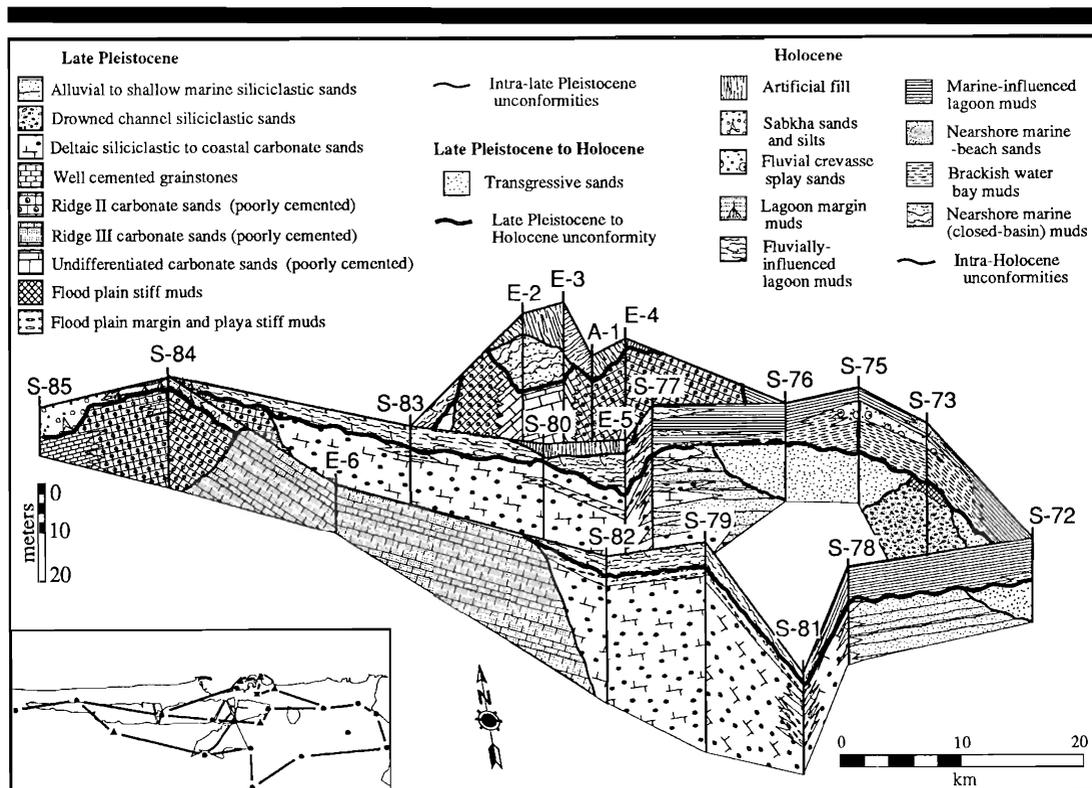
Figure 13.  Stratigraphic fence diagram summarizing the late Pleistocene and Holocene lithofacies distributions in time and space.

(2) Well cemented grainstones occur locally within poorly cemented Ridge II and Ridge III carbonate sands (Figures 13, 14A–A'). Initial petrologic analysis indicates at least two generations of cement (STANLEY and HAMZA, 1992).

(3) Deltaic siliciclastic to coastal carbonate sands of late Pleistocene age (>38,000–15,000 years BP) occur in the central portion of the study area (Figures 13, 14A–A'). These sands mark the transition zone between the Nile delta to the east and the desert coast to the west. Unconformities separate the deltaic siliciclastic to coastal carbonate sands from the significantly older Ridge II and Ridge III carbonates.

(4) Thick sections of late Pleistocene siliciclastic alluvial sands (>35,000–12,700 years BP) occur in the eastern part of the study area. These medium to coarse, quartzose sands are interpreted to be braided river deposits, with some intercalated nearshore marine and beach sands. These sands are the westernmost portion of the thick and widespread Nile sand lithosome of late Pleis-

tocene age (ATTIA, 1954; SAID, 1981; COUTELLIER and STANLEY, 1987; ARBOUILLE and STANLEY, 1991; STANLEY et al., 1992; CHEN et al., 1992).

(5) A thick section of drowned channel sands (>13,000 years BP) occurs in the lower portion of core S-73, to the east of Abu Sir ridge (Figures 13, 14A–A'). These very coarse sands record the location of a major Pleistocene (pre-Canopic) Nile channel. Absence of incised river channels through Abu Sir Ridge II (>35,000 years BP) to the west of S-73 (Figures 2, 4) indicates that this pre-Canopic channel was the westernmost River Nile distributary during the latest Pleistocene.

(6) Late Pleistocene stiff muds (>35,000–11,000 years BP) occur in the upper portions of many late Pleistocene sand sequences (Figures 13, 14A–A'). These muds are interpreted to be overbank and playa deposits which accumulated in localized depressions during seasonal floods. It is of note that these stiff muds are most common in the central portion of the study area (Maryut lake region); this indicates that the lake sector was a
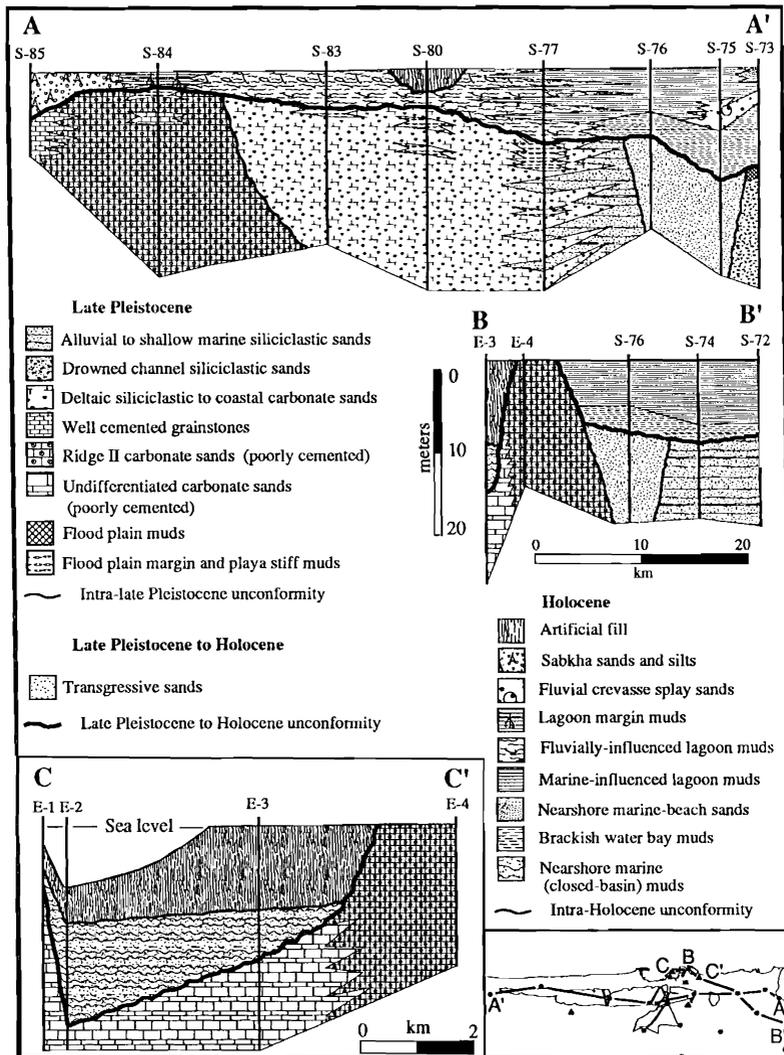
Figure 14.   Stratigraphic cross-sections showing late Pleistocene and Holocene lithofacies distributions in three sectors of study area. Note that section C-C' has a different horizontal scale than A-A' and B-B'.

depression during late Pleistocene as well as Holocene times.

(7) Late Pleistocene to early Holocene shallow marine transgressive sands occur in the eastern study area (Figures 13, 14A–A'). These sands overlie older late Pleistocene alluvial sands and muds (COUTELLIER and STANLEY, 1987; ARBOUILLE and STANLEY, 1991; STANLEY et al., 1992; CHEN et al., 1992). Transgressive sands terminate near the southern margin of the modern Idku lagoon, and record the southwestern limit of the

late Pleistocene to early Holocene (Flandrian) marine transgression. An unconformity occurs at the base of the transgressive sands and is the result of wave reworking of older, late Pleistocene deposits.

(8) An unconformity also occurs at the base of the Holocene section throughout the study area. Holocene deltaic and coastal sediments began to accumulate above the hiatus ~7,500 years ago as the rate of sea-level rise markedly decelerated.

(9) Radiometric dates indicate that onset of

Holocene sedimentation above the hiatus occurred earlier in the eastern sector than in the western sector of the study area. The absence of early Holocene sediments in the west may be attributed to emergence of that region during that time (Figure 11A).

(10) Holocene sequences above the unconformity thin from northeast to southwest across the study area (Figures 11, 14A–A') which also suggests emergence in the south and west.

(11) Holocene sediments tend to be marine coastal in the east and terrestrial in the west. It is of note that no open marine, deep water facies (e.g., prodelta and delta-front) of Holocence age occur in the study area.

(12) Middle and late Holocene lagoon deposits occur throughout the study area and demonstrate that, until recently, coastal wetlands were the predominant ecosystem of the northwestern Nile delta plain.

(13) Holocene lagoon deposits are marine-influenced in the east and fluvially-influenced in the south and west. Differences between these two subfacies are subtle and the transition between them is highly gradational.

(14) Holocene fluvial sands interfinger with brackish water bay and lagoon muds in the eastern portion of the study area (Figures 13, 14A–A'). These sands were deposited by the former Canopic channel (CHEN et al., 1992).

(15) The Holocene sabkha and alluvial fan deposits, in core S-85 (Figures 13, 14A–A'), are interpreted to have accumulated near the edge of Lake Mareotis along the northern slopes of Ridge III.

(16) Holocene nearshore marine (closed-basin) muds in the harbor district of Alexandria were deposited in a basin which was separated from the Maryut depression by Ridge II (Figures 13, 14B–B'). This basin has subsided nearly 25 m (rates of ~0.3 cm/yr) during Holocene time (Figure 14C–C'). These subsidence rates are the highest in the study area and are comparable to rates in the Rosetta promontory to the east (CHEN et al., 1992). It is of note that the barrier that separates the Eastern and Western harbors is artificial (JONDET, 1916; MORCOS, 1985) which implies that the two Holocene sediment wedges in the harbor area (Figure 11) were once united.

(17) Thick sections of artificial fill in the upper parts of borings S-80 and E-1 to E-5 are yet another indication of extensive alteration of this region by human activity.

## EVOLUTION OF LAKE MAREOTIS AND MODERN MARYUT LAKE

### Early History

Lake Mareotis, precursor of Maryut lake, was the largest geomorphic feature in the study area during the middle and late Holocene. Prior to this time, the region was a subaerially-exposed depression bound to the northwest by elevated carbonate Ridge II. During the late Pleistocene, when sea level was generally lower, most of this pre-Mareotis basin was a seasonally flooded alluvial plain in which calcareous and gypsiferous sandy muds accumulated (CHEN and STANLEY, in press).

Radiocarbon-dated core sections indicate that Lake Mareotis had developed by at least 6,100 years BP. At about that time, climate was becoming more arid so that grasslands of the Libyan desert to the southwest were disappearing, prompting herdsmen to immigrate to the more temperate Mareotis region (DE COSSON, 1935). By ~5,000 years ago, the Lake Mareotis region was an important fishing and agricultural center, as well as the first major port of the early dynasties of Egypt (NEWBERRY, 1908). Historic records indicate that early Mareotis was a freshwater lake (DE COSSON, 1935); however, analysis of molluscan faunas demonstrates that the lake was more likely a mixed freshwater-brackish water body (M.P. BERNASCONI, written communication, 1992).

From ~6,000 to 800 years BP, the surface of Lake Mareotis was at about sea level and covered ~700 km², extending more than 40 km southeast of Alexandria and 70 km southwest between Ridges II and III, beyond Abu Sir (Figure 15). Archeological records show that lake depths during this period were sufficiently deep that ships could enter from the River Nile, traverse the lake and dock at southern Alexandria, and even at Abu Sir (DE COSSON, 1935). Our analysis indicates that Lake Mareotis was deeper than the other Nile delta coastal water bodies because (1) large volumes of River Nile sediments were not delivered to this depression and (2) the region was locally subject to subsidence.

It remains unclear from historic records how and where Lake Mareotis was supplied with marine and fresh water. Maps older than 2,000 years (e.g., those of Herodotus and Strabo) do not show any channel or canal connecting the River Nile with Lake Mareotis (TOUSSOUN, 1922; SAID, 1981). More recent maps (such as that of Serapion), however, show a canal extending from the Canopic
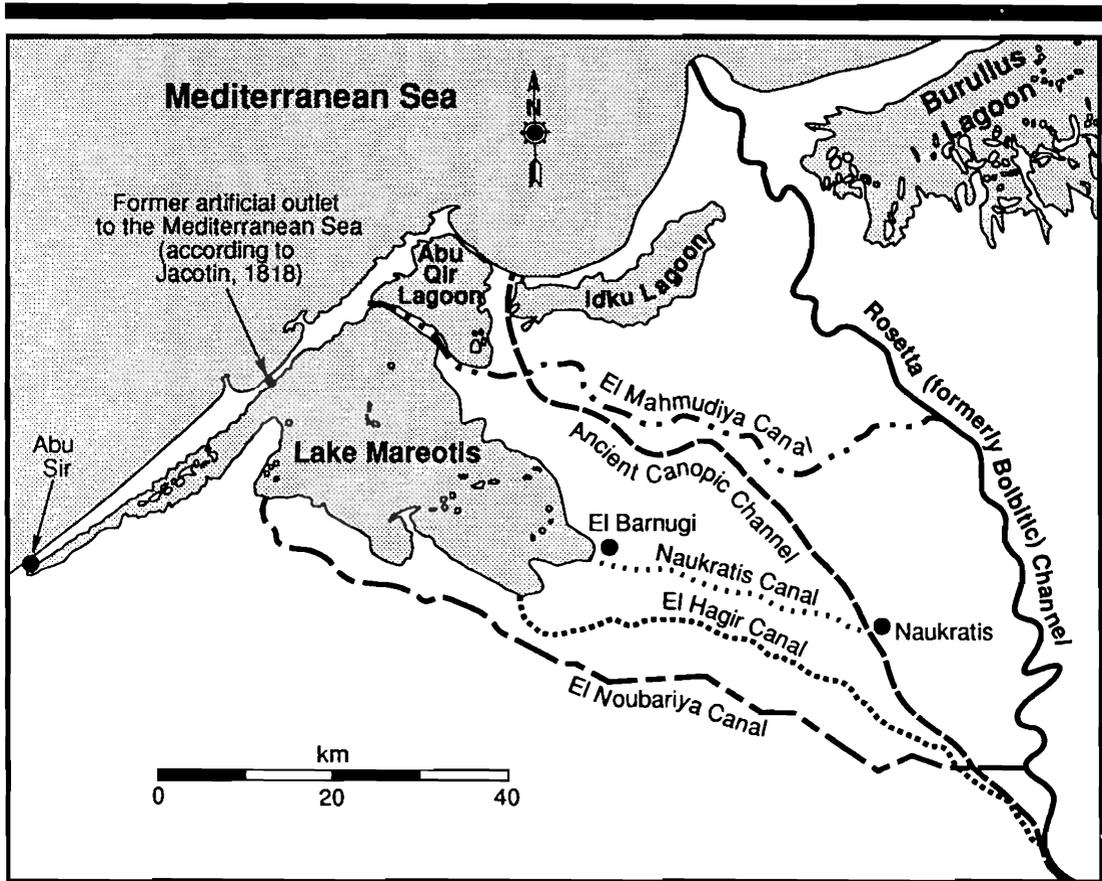
Figure 15.  Map of the northwest Nile delta showing (1) extent of former Lake Mareotis, (2) trace of former Canopic channel, (3) artificial outlet near El Max, (4) trace of two branches (El Hagir and Naukratis canals) of the former Canopic channel which supplied River Nile water to Lake Mareotis, (5) location of the ancient Greek city of Naukratis and (6) present-day El Noubariya and El Mahmudiya canals. Outline of lagoons is modified from Jacotin (1818).

channel to the southeast end of the lake. Maps of the early nineteenth century also show a canal extending from the Rosetta channel to the lake (ARROWSMITH, 1802, 1807; DU BOIS-AYMÉ, 1813; JACOTIN, 1818). According to DE COSSON (1935), it is generally accepted that a canal extended from the city of Naukratis to the southeast end of Lake Mareotis, near the village of El Barnugi (Figure 15). He also suggested that a second channel followed the course of El Hagir canal. An artificial outlet through Ridge II near El Max (whose base was slightly above sea level) prevented Lake Mareotis from overfilling and endangering the Alexandria region during floods (JACOTIN, 1818; SHAFEI, 1952).

Petrologic data analyzed in the present study indicate that from ~6,000 to 800 years ago, Lake Mareotis was connected to the River Nile, and that there were periodic incursions of marine water resulting in brackish conditions. Significant fluvial input into the region is suggested by the frequency distribution of light minerals (mostly quartz), the dominant sand component throughout most of the study area (Figure 8D). Notable proportions of heavy minerals and mica (Figure 10A and B) also record terrigenous input; their distributions indicate input was predominantly from the southeast. High proportions of shell and shell fragments (Figure 8C) indicate that terrigenous sediment input was sufficiently low that shell-forming organisms proliferated. The presence of verdine/glauconite and foraminifera (Figure 10C and D) indicate that Lake Mareotis experienced at least some marine influx; frequency

distributions of these two components indicate marine waters entered from the northeast. Low proportions of vegetal matter in core samples (Figure 10E) suggest that these borings were recovered from what were once the central, deeper portions of Lake Mareotis, which were at some distance from lake margins and marsh plant thickets.

Historic records indicate that all canals linking Lake Mareotis to the Canopic and Rosetta channels silted up by the twelfth century so that lake levels fell and the region became a series of salt lakes and sabkhas. Without a fresh water supply, Alexandria declined in importance until Mohamed Ali Pasha reconstructed El Mahmudiya canal in 1820. Because Maryut depression did not receive water from Abu Qir lagoon or El Mahmudiya canal, lake levels remained low, except from 1801 to 1804 and 1807 to 1808. At these two times, the dyke between Maryut depression and former Abu Qir lagoon was breached for tactical military purposes, and the depression filled with sea water (DE COSSON, 1935).

It is of note that the early nineteenth century maps of ARROWSMITH (1802, 1807), DU BOIS-AYMÉ (1813) and JACOTIN (1818) portray Maryut during its brief period of inundation by the sea. However, in 1808 the barrier between Maryut and Abu Qir lagoon was restored and the lake dried up again until 1892 when the irrigation sytem of the Beheirah district (northwestern Nile delta) was organized and several canals flowed into, and once again filled the depression with water, creating Maryut lake. Later, pumps were installed at El Max to control the size of the lake by keeping levels at about 2.8 m below sea level.

## Recent Evolution of Maryut Lake and the Role of Man

Modern Maryut lake levels are still maintained at ~2.8 m below sea level by pumping from the lake to the sea at El Max. The lake currently covers ~90 km² which is 13% of the size it would be if the water surface was at sea level. The central portions of Maryut lake (the northern, southeastern, southern, southwestern, central and east-central sub-basins in Figure 6) receive most of its water from El Qalaa drain (Figures 1, 2). It also receives water from El Umoum drain through several breaks in the embankment separating the drain course from the lake. Maryut lake is the receptacle for large volumes of untreated industrial wastes from El Qalaa drain, and sewage and

industrial wastes from several outfalls in the northeastern sector of the lake. Untreated wastes have rendered Maryut lake highly polluted and partially eutrophic (WAHBY et al., 1978; ABDEL-KADER, 1982; SAAD et al., 1984). Once highly productive, fishing yields have declined from 7,000 tons in 1962 to 1,000 tons in 1978, mainly because of pollution (WAHBY et al., 1978). Nonetheless, the lake supplies ~22% of the fish caught in Egypt's brackish water lakes and lagoons (ABOUL DAHAB et al., 1990).

Several investigators (e.g., ALEEM and SAMAAN, 1969a; EL-WAKEEL and WAHBY, 1970; SAAD, 1972; WAHBY et al., 1978; SAAD et al., 1982) recognized four Maryut lake sub-basins which are separated by artificial embankments (Figure 6, inset). With construction of more canals and causeways, these four sub-basins have been further subdivided into >6 sub-basins (Figure 6). In addition to these six sub-basins, the Hydrodrome, west-central and western sub-basins are considered to be part of the Maryut depression (Figure 4) because they are subsea-level water bodies that were once part of Lake Mareotis (DE COSSON, 1935). To record the extensive influence of man and to document the accelerating changes affecting Maryut, that could serve for future reference, a brief description of each of the nine Maryut sub-basins is given below.

El Nouzha Hydrodrome sub-basin is ~4.8 km² with an average bottom depth of 3.65 m below sea level, and water surface level maintained at about 0.6 m below sea level. Chlorosities are quite low and range from 0.1 to 0.4 g/l (KERAMBRUN, 1986). The Hydrodrome was separated from Maryut lake in the late 1930's to form a seaplane airport (SAAD et al., 1985). It receives its water from the relatively unpolluted Mahmudiya canal. The Hydrodrome sub-basin currently serves as a fish farm (KERAMBRUN, 1986).

The northern sub-basin is ~29.4 km² with depths between 0.9 and 1.5 m, and chlorosities between 1.1 and 2.6 g/l (KERAMBRUN, 1986). This sub-basin is heavily polluted by industrial wastes from El Qalaa drain, and untreated sewage from municipal and industrial outfalls (ALEEM and SAMAAN, 1969a; EL-WAKEEL and WAHBY, 1970; SAAD, 1972, 1983a,b; SAAD, 1980; WAHBY and ABDEL MONEIM, 1979; MITWALLY, 1982; SAAD et al., 1981; SAAD et al., 1982; SAAD et al., 1984; SAAD et al., 1985). Moreover, the eastern and southeastern margins of this sub-basin are solid waste disposal sites for the city of Alexandria (Figure 2). Two

other sources of pollution in this sub-basin are the El Noubariya canal (such as tin from paint of barges and ships; ABOUL DAHAB et al., 1990) and air (including mercury fallout from industries at El Max and El Dekheila; ELSOKKARY, 1989). Bottom sediments are generally dark gray (N3) clayey silt in the northeastern, and shelly silt and clay in the remainder of the sub-basin (EL-WAKEEL and WAHBY, 1970; SAAD, 1980). These sediments contain large amounts of $H_2S$. In the western portion of this sub-basin, floating *Phragmites* and *Typha* thickets are widespread; these thickets are currently being cleared to accommodate fish ponds.

The southeastern sub-basin is ~4.2 km² with water depths of 0.9 to 1.5 m, and chlorosities of 1.1 to 2.6 g/l (KERAMBRUN, 1986). This sub-basin is relatively unpolluted and serves as a fish farm (WAHBY et al., 1978). Bottom sediments are primarily composed of dark gray (N3) shelly silt and clay (EL-WAKEEL and WAHBY, 1970). This sub-basin has some floating thickets at its western end (Figure 2).

The southern and southwestern sub-basins (the southwestern basin of ALEEM and SALAAM, 1969a) cover ~12.6 km², and are partially divided by El Noubariya canal, although breaks in the canal embankments allow water to pass from one sub-basin to the other. Water depths are ~0.9 to 1.5 m, and chlorosities are 1.1 to 2.6 g/l. Bottom sediments are primarily dark gray (N3) shelly silt and clay, and silty clay (EL-WAKEEL and WAHBY, 1970). Large portions of these two sub-basins are covered with floating thickets of *Phragmites* and other marsh plants. Subaqueous macroscopic algae is also common (ALEEM and SALAAM, 1969b). The southern portion of the southwestern sub-basin is industrialized; ABDEL-KADER (1982) recorded considerable wetland loss in this portion of the sub-basin.

The central and east-central sub-basins (the northwest basin of ALEEM and SALAAM, 1969a) cover ~8.4 km². These two sub-basins are partially separated by a canal; however, breaks in the canal embankments permit passage from one sub-basin to the other. Their relatively unpolluted waters have depths of 1 to 1.5 m and chlorosities of 1.1 to 2.6 g/l (KERAMBRUN, 1986). Bottom sediments are primarily dark gray (N3) shelly silt and clay (EL-WAKEEL and WAHBY, 1970). These two sub-basins are primarily open water lakes, but the northern portion of the east-central sub-basin is marshy. The northern end of the central, and

the southern end of both the east-central and central sub-basins are industrialized. The west end of the central sub-basin is a continuous embankment, so that waters of the central and west-central sub-basins do not mix.

The west-central sub-basin is ~35 km² and is a commercial salt pond which produces ~1,000,000 kg of unrefined salt per year (H.Z. HANAH, personal communication, 1992). Water is maintained at salinities of 92 g/l in the main body of this sub-basin (Figure 5I); concentrations are regulated by adding Mediterranean seawater through two underground pipes. The color of this brine is light red (5R 6/6), from red algae cysts (*Artemia*) and microscopic shrimp. The 92 g/l brine is dried and salt extracted in fifteen shallow pans (H.Z. HANAH, personal communication, 1992).

The western sub-basin, segregated on the southwest and northeast ends by causeways (Figures 2, 6) is a complex of sabkhas and shallow playas whose relative size varies according to season. The western sub-basin receives its waters from groundwater seepage and runoff. The surface of this sub-basin is dry for much of the year (especially in the summer). Sediments from this sub-basin generally include halite and gypsum crusts at the surface (during the dry season) and gypsiferous loess below. Pelecypod (*Cardium*) fossils are common, and are relics of former Lake Mareotis (DE COSSON, 1935; ALI and WEST, 1983). The floor of the western sub-basin is generally flat and sparsely covered with halophytic plants. A commercial fish pond has been constructed at the northeast end of the sub-basin (Figure 2).

Maryut lake and associated wetlands continue to be reduced in size by land reclamation projects and subdivision by canals and causeways. It is also of serious concern that large portions of the lake are increasingly polluted with industrial and municipal wastes. These actions have resulted in a significant decrease in the lake fish productivity and are contributing to increased health hazards for the region.

## PALEOGEOGRAPHY AND CONCLUSIONS

Subsurface distribution of late Pleistocene and Holocene lithofacies in the Alexandria region have been defined on the basis of petrologic, biogenic and radiometric analyses, and remote sensing. A paleogeographic synthesis is derived from integration of these data with the well-documented archeologic record of the Alexandria region. Of particular concern are factors which control sed-
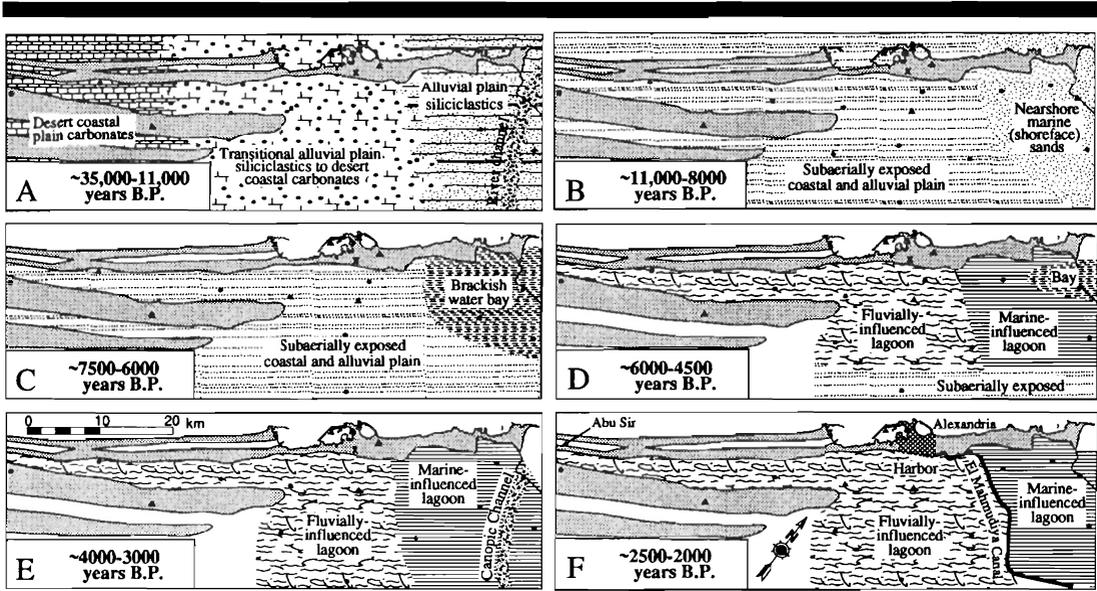
Figure 16.    Series of time-slice paleogeographic maps showing late Pleistocene to recent evolution of northwestern Nile delta and adjacent coastal region near Alexandria (explanation in text).

iment distribution, that is sea level, tectonism, climate, sedimentary processes and, more recently, man.

With regard to late Pleistocene deposits and their distribution, this study has focused on the origin of: (1) siliciclastic sands in the eastern, mixed siliciclastic-carbonate sands in the central and carbonate sands in the western sector of the study area, (2) stiff muds and (3) paleochannel systems.

Facies analysis reveals that marine transgressive sands of latest Pleistocene to Holocene age are localized in the eastern sector of the study area. Moreover, distributions of Holocene sections show: (1) brackish water bay muds in the northeast, (2) fluvial sands in the east, (3) marine-influenced muds in the east and fluvially-influenced muds in the southwest, (4) carbonate-rich sabkha and alluvial fan sands in the west, and (5) reduced depositional sequences in the southern and western sectors.

Mapping of subsurface lithofacies and paleoenvironments is useful for interpreting geomorphic features in the Alexandria region, such as: (1) the distinctive coast which includes siliciclastic sand flats in western Abu Qir bay, seacliffs and pocket beaches from Abu Qir to El Dekheila, and extensive, oolitic beaches from El Dekheila to Abu Sir; (2) kôms to the south of Ridge III; (3) sabkhas in inner ridge depressions; and (4) semidesert in the

southwest. Paleogeographic analysis also serves to differentiate the relative influence of natural and anthropogenic factors on sedimentation, and thus provides a means to better evaluate man's role on the Alexandria region at present and in the future.

During the late Pleistocene, prior to 35,000 years BP (Sicilian to late Monasterian), a series of prominent nearshore marine to coastal dune ridges were deposited in this region. These carbonate-rich sands accumulated during a series of sea-level highstands. Minor sea-level fluctuations affected the development of each ridge, and resulted in intermittent subaerial exposure and subsequent caliche and paleosol development. During time of ridge formation, back-barrier lagoons and sabkhas developed in depressions on the landward side of the ridges; mud and gypsum accumulated in these depressions. The entire ridge complex has been subsequently uplifted and tilted to the north and northeast.

Evolution of the Alexandria region during the past ~35,000 years is summarized in a series of time-slice paleogeographic maps (Figure 16).

From ~35,000 to 11,000 years BP, the coast in the Alexandria region migrated seaward from near its present location to as much as 20 km to the northwest (near the shelfbreak) during the latest Pleistocene lowstand (~20,000–18,000 years BP),

and then landward (southeastward) to about the present-day midshelf. During this period, the area was a subaerially exposed coastal and alluvial plain. A NNW-trending, primarily braided river channel system (pre-Canopic) flowed across the alluvial plain to the present-day shelf edge (MAL-DONADO and STANLEY, 1979). The major river channel was periodically inundated by brackish water during intermittent sea-level rises (CHEN *et al.*, 1992). This was the westernmost channel complex of the River Nile system during the late Pleistocene. The mixed siliciclastic-carbonate sands in the central study area record the transition from alluvial plain to the east and desert coastal plain to the west. The Maryut region was a depression during this period in which relatively thick and widespread floodplain sandy muds accumulated. Gypsum and calcareous nodules, and the physical properties of these muds, record alternating wet and dry conditions in a generally arid climate (CHEN and STANLEY, in press).

From ~11,000 to 8,000 years BP, the coast migrated from the present-day midshelf landward (southeastward) as sea level continued to rise rapidly. As shoreline transgressed landward, late Pleistocene sediments were reworked by coastal waves and currents which resulted in deposition of nearshore marine shoreface and beach sands. Rapidly rising sea level caused the shoreline to transgress into the eastern part of the study area. Eventually, the rate of sea-level rise began to decelerate, transgression halted and much of the region became a surface of nondeposition (and probably erosion in the south and west). Available subsurface data do not provide information about river channels in the study area during this period. The climate was generally more humid at this time.

At ~7,500 years BP, the rate of sea-level rise began to decelerate, and brackish water bay and lagoon muds accumulated in the eastern portion of the study area. Most of the region to the south and west remained subaerially exposed in a relatively humid climate.

By ~6,000 years BP, much of the area was covered by brackish and fresh water. The central portion of the region was a fluvially-influenced lagoon (Lake Mareotis), whereas the eastern portion evolved into a marine-influenced lagoon. The fluvially-influenced portion of the lagoon was fed by one or more minor branches of the Canopic channel which flowed into the southeastern portion of the lagoon (Figure 15). These minor branches carried only a fraction of the sediment load of the Canopic branch and thus Lake Mareotis remained a sediment-starved deep water lagoon. During this period, the climate was becoming more arid.

By ~4,000–3,000 years BP, sea level steadily rose to ~3–4 m below its present level. As the result of rising sea level and subsidence, Lake Mareotis spread further to the south. During this time, the Canopic branch migrated westward as far as the eastern margin of Abu Qir lagoon, just east of Abu Sir Ridge II. It is of note that the course of the channel during this period nearly coincided with the course of the late Pleistocene, pre-Canopic channel. Although climate had become arid, the southwestern portion of the study area was a thriving agricultural region (DE COSSON, 1935).

By ~2,000 years BP, the Canopic branch was diminishing as a significant Nile distributary, and the Rosetta (Bolbitic) branch was being artificially excavated (*cf.* SAID, 1981). However, Lake Mareotis continued as a deep, mostly fresh water lake, perhaps the result of excavation of the canal between the city of Naukratis and the lake (*cf.* DE COSSON, 1935). Alexandria had become a major eastern Mediterranean port, with harbors on both Lake Mareotis and the Mediterranean Sea. El Mahmudiya canal had been constructed by this time and may have isolated the fluvially- from the marine-influenced portion of the lagoon. A system of wells and cisterns was constructed in the southwestern portion of the study area to enhance agricultural output in this arid region.

By 800 years BP (1200 AD), the Canopic branch and El Mahmudiya canal had filled with silt so that the supply of fresh water to the Alexandria region was markedly diminished. As a result, Mareotis lake level fell and the depression became the site of salt lakes and sabkhas. Alexandria declined in importance as a port and trade center. The once-rich agricultural regions to the south and west of Alexandria disappeared as the result of increasing aridification and decay of the Greco-Roman system of wells and cisterns (DE COSSON, 1935). Fresh water was reintroduced into Maryut depression in the late nineteenth century by diverting artificial drains to this region. Lake levels are currently maintained at nearly 3 m below sea level by pumping water from the lake to the Mediterranean sea. Large portions of Maryut lake, and all of Abu Qir lagoon, have been drained and are currently being cultivated.

In summary, the present study demonstrates that the boundary between the Nile fluvial system to the east and the desert coastal region to the west has not significantly shifted since late Pleistocene time. During the mid- to late Holocene, Lake Mareotis was a fluvially-influenced lagoon and, therefore, an integral part of the Nile delta system. The western edge of the Nile delta is now obscured by irrigation projects which have artificially expanded the cultivated surface westward and southwestward onto former desert.

This investigation reveals that the Alexandria sector has been increasingly controlled by man and that the anthropogenic factor is now the dominant control on coastal plain evolution and depositional patterns. Unlike other Nile delta sectors to the east where natural factors are the dominant control on the evolution of the Nile coastal region, it seems inevitable that wetland loss will continue and pollution increase as the Alexandria region copes with its rapidly growing population and increasing industrialization. Natural factors are also of serious consideration. It may be necessary, for example, to augment coastal structures along the Abu Qir bay coast to prevent marine inundation into low lying regions. Even then, marked accentuation in sea-level rise, land subsidence or earthquake activity could result in inundation of Abu Qir and Maryut depressions. Saline groundwater incursion in low-lying regions is likely to increase.

Fortunately, the expanding Abu Qir-Alexandria-El Dekheila-El Agami urban center is positioned on a carbonate ridge which lies several meters above sea level. Expansion of irrigation projects into desert (which is well above sea level) to the south and southwest of Alexandria is a reasonable course of action for future development of this region.

## LITERATURE CITED

ABDEL-KADER, A., 1982. Landsat Analysis of the Nile Delta, Egypt. M.Sc. Thesis, Univ. of Delaware, Newark, Delaware, 260p.

ABDEL-MOATI, A.R. and EL-SAMMAK, A.A., 1988. Geochemistry of short core sediments off Alexandria region. *Rapports et Procès-verbaux des Réunions, Commission Internationale pour l'Exploration Scientifique de la Mer Méditerranée*, 31.2, 107.

ABDEL WAHAB, H.S. and STANLEY, D.J., 1991. Clay mineralogy and the recent evolution of the north-central Nile delta, Egypt. *Journal of Coastal Research*, 7, 317–329.

ABOUL DAHAB, O.A., 1988. Speciation of tin compounds in sediments of the Alexandria coast belt. *Water, Air, and Soil Pollution*, 40, 433–441.

ABOUL DAHAB, O.A.; EL-SABROUTI, M.A., and HALIM, Y., 1990. Tin compounds in sediments of Lake Maryut, Egypt. *Environmental Pollution*, 63, 329–344.

ABU-ZEID, M.M. and STANLEY, D.J., 1990. Temporal and spatial distribution of clay minerals in Late Quaternary deposits of the Nile delta, Egypt. *Journal of Coastal Research*, 6, 677–698.

ADAMSON, D.A.; GASSE, F.; STREET, F.A., and WILLIAMS, M.A., 1980. Late Quaternary history of the Nile. *Nature*, 288, 50–55.

ALEEM, A.A. and SAMAAN, A.A., 1969a. Productivity of Lake Mariut, Egypt. Part I. Physical and chemical aspects. *Internationale Revue der Gesamten Hydrobiologie*, 54(3), 313–355.

ALEEM, A.A. and SAMAAN, A.A., 1969b. Productivity of Lake Mariut, Egypt. Part II. Primary production. *Internationale Revue de Gesamten Hydrobiologie*, 54 (4), 491–527.

ALEXANDERSSON, T., 1990. Holocene shelf sedimentation on the western Egyptian shelf. *Rapports et Procès-verbaux des Réunions, Commission Internationale pour l'Exploration Scientifique de la Mer Méditerranée*, 31.2, 108.

ALI, Y.A. and WEST, I., 1983. Relationships of modern gypsum nodules in sabkhas of loess to compositions

of brines and sediments in northern Egypt. *Journal of Sedimentary Petrology*, 53(4), 1151–1168.

ANWAR, Y.M.; EL ASKARY, M.A., and NASR, S.M., 1981. Petrography and origin of the oolitic carbonate sediments of Arabs' Bay, western part of the continental shelf of Egypt. *Neues Jahrbuch fuer Geologie und Palaeontologie. Monatshefte*, 1981(2), 65–75.

ARBOUILLE, D. and STANLEY, D.J., 1991. Late Quaternary evolution of the Burullus lagoon region, north-central Nile delta, Egypt. *Marine Geology*, 99, 45–66.

ARROWSMITH, A., 1802. *Plan of the Operations of the British and Ottoman Forces in Egypt.* London (map, 1 sheet).

ARROWSMITH, A., 1807. *A Map of Lower Egypt from Various Surveys Communicated by Major Bryce and Other Officers.* London (map, 1 sheet).

ATTIA, M.I., 1954. *Deposits in the Nile Valley and the Delta.* Cairo: Geological Survey of Egypt, 356p.

BALL, J., 1939. *Contributions to the Geography of Egypt.* Cairo: Survey and Mines Dept. 308p.

BELL, B., 1970. The oldest records of Nile floods. *The Geographical Journal*, 136, 569–573.

BERNASCONI, M.P.; STANLEY, D.J., and DI GERONIMO, I., 1991. Molluscan faunas and paleobathymetry of the Holocene sequences in the Nile delta, Egypt. *Marine Geology*, 99, 29–43.

BLANCKENHORN, M., 1901. Neues zur Geologie und Palaeontologie Aegyptens, IV: Das Pliocän und Quartärzeitalter in Aegypten ausschliesslich des Rothen Meergebietes. *Zeitschrift. Deutsche Geologische Gesellschaft*, 53, 307–502.

BLANCKENHORN, M., 1921. *Handbuch der Regionalen Geologie: Aegypten.* Heidelberg: Carl Winters Universitätsbuchhandlung, 244p.

BROUSSARD, M.L., Editor, 1975. *Deltas, Models for Exploration.* Houston, Texas: Houston Geological Society, 555p.

BUTZER, K.W., 1960. On the Pleistocene shorelines of Arabs' Gulf, Egypt. *Journal of Geology*, 68, 626–637.

BUTZER, K.W., 1976. *Early Hydraulic Civilization in Egypt.* Chicago: University of Chicago Press, 134p.

CHEN, Z. and STANLEY, D.J., 1993. Alluvial stiff muds (Late Pleistocene) underlying the lower Nile Delta plain: Petrology, stratigraphy and origin. *Journal of Coastal Research*, 9(2).

CHEN, Z.; WARNE, A.G., and STANLEY, D.J., 1992. Late Quaternary evolution of the northwest Nile delta between Rosetta and Alexandria, Egypt. *Journal of Coastal Research*, 8, 527–561.

CHERIF, O.H.; EL-SHEIKH, H., and LABIB, F., 1988. The foraminifera of the Pleistocene coastal ridges of the area to the west of Alexandria, Egypt. *Revue de Paléobiologie*, 2, 735–740.

COLEMAN, J.M., 1982. *Deltas: Processes of Deposition and Models for Exploration* (2nd Edition). Boston, Massachusetts: International Human Resources Development Corp., 124p.

COLLINSON, J.D., 1986. Alluvial sediments. *In:* Reading, H.G. (ed.), *Sedimentary Environments and Facies.* Boston, Massachusetts: Blackwell, pp. 20–62.

COUTELLIER, V. and STANLEY, D. J., 1987. Late Quaternary stratigraphy and paleogeography of the eastern Nile delta, Egypt. *Marine Geology*, 77, 257–275.

DE COSSON, A., 1935. *Mareotis.* London: Morrison and Gibb, Ltd., 219p.

DI GERONIMO, I. and ROBBA, E., 1976. Metodologie qualitative e quantitative per lo studio delle biocenosi e delle paleocomunita marine bentoniche. *C.N.R. Gruppo Paleobenthos, Rapporto de Lavoro*, n.1, 1–35.

DOWIDAR, N.M. and ABOUL KASSIM, T.A., 1986. Levels of nutrients and chlorophyll biomass in a highly polluted basin, the Eastern Harbour of Alexandria. *Rapports et Procès Verbaux de Réunions, Commission Internationale pour l'Exploration Scientifique de la Mer Méditerranée*, 30.2, 33.

DU BOIS-AYMÉ, M., 1813. Mémoire sur les anciennes branches du Nil et ses embouchures dans la mer. *Description de l'Egypte, Antiquités, Mémoires*, I, 277–290.

EL FAYOUMY, I.F.; EL SHAZLI, M.M., and HAMMAD F.A., 1975. *Geomorphology of the Coastal Area Between Abu Qir and Rasheed (Northwest of the Nile Delta, E.A.R.).* Cairo: Faculty of Science, Cairo University Press, pp. 135–147.

EL-FISHAWI, N.M. and FANOS, A.M., 1989. Prediction of sea level rise by 2100, Nile delta coast. *INQUA Commission on Quaternary Shorelines Newsletter*, 11, 43–47.

EL RAMLY, I.M., 1968. Quaternary shoreline changes relative to paleoclimates and their emphasis on groundwater possibilities of the El Amiriya/El Alamein district, Western Desert, Mediterranean littoral, U.S.R. *Bulletin de l'Institut d'Egypte*, 49, 163–166.

EL RAMLY, I.M., 1971. Shoreline changes during the Quaternary in the Western Desert Mediterranean coastal region (Alexandria–Sallum), U.A.R. *Quaternaria*, 15, 285–292.

EL-RAYIS, O. and SAAD, M.A.H., 1986. Origins of trace elements in a main land-based source on the North African coast, west of the Nile Delta. *Rapports et Procès Verbaux de Réunions, Commission Internationale pour l'Exploration Scientifique de la Mer Méditerranée*, 30.2, 33.

EL-RAYIS, O.; SAAD, M.A.H., and EL-NADY, F., 1986. Accumulating mechanisms of metals in surface sediments of a coastal bay on the North African coast. *Rapports et Procès Verbaux de Réunions, Commission Internationale pour l'Exploration Scientifique de la Mer Méditerranée*, 30.2, 65.

EL-SAMIE, A.G.A., 1960. Soil survey, classification and management of the Mariut Agricultural Project. *Bulletin of the Egyptian Geographical Society*, 33, 147–176.

EL-SAYED, M.K., 1979. The inner shelf off the Nile delta: Sediment types and depositional environments. *Oceanologica Acta*, 2, 249–252.

EL-SAYED, M.K., 1988a. Progressive cementation in Pleistocene carbonate sediments along the coastal area of Alexandria, Egypt. *Journal of Coastal Research*, 4, 289–299.

EL-SAYED, M.K., 1988b. Sea level rise in Alexandria during the late Holocene: Archaeological evidences. *Rapports et Procès Verbaux de Réunions, Commission Internationale pour l'Exploration Scientifique de la Mer Méditerranée*, 31.2, 108.

EL-SAYED, M.K., 1988c. Application of factor analysis to the geochemical data of Alexandria shelf sediments. *Rapports et Procès Verbaux de Réunions,*

Commission Internationale pour l'Exploration Scientifique de la Mer Méditerranée, 31.2, 108.

EL-SAYED, M.K.; EL-WAKEEL, S.K., and RIFAAT, A.E., 1988. Factor analysis of sediments in the Alexandria Western Harbour, Egypt. Oceanologica Acta, 11(1), 1–11.

EL-SHAHAT, A.; SAYED, A.; HEGAB, O., and EL-HEFNAWI, M.A., 1987. Petrography and chemistry of some calcretes from the northwestern coastal plain of Egypt. Egyptian Journal of Geology, 31, 161–180.

EL SHAMI, I.; EL SHAZLY, M., and SHATA, A., 1971. Contribution to the geology of El Dabaa area "Western Mediterranean Littoral Zone." Desert Institute Bulletin, U.A.R., 19, 63–93.

EL SHAZLY, E.M.; ABDEL-HADY, M.A.; GHAWABY, M.A.; EL KASSAS, I.A.; KHAWASIK, S.M.; EL SHAZLY, M.M., and SANAD, S., 1975. Geologic Interpretation of Landsat Satellite Images for West Nile Delta Area, Egypt. The Remote Sensing Research Project, Academy of Scientific Research and Technology, Cairo, Egypt, 44p.

ELSOKKARY, I.H., 1989. Contamination of the terrestrial ecosystem by mercury around the industrial complex center of el Max, western area of Alexandria. In: Vernet, J.-P. (ed.), International Conference: Heavy Metals in the Environment, 2, 321–324.

EL-WAKEEL, S.K., 1964. Recent bottom sediments from the neighborhood of Alexandria, Egypt. Marine Geology, 2, 137–146.

EL-WAKEEL, S.K.; ABDOU, H.F., and WAHBY, S.B., 1970. Foraminifera from bottom sediments of Lake Maryut and Lake Manzalah, Egypt. Bulletin of the Institute of Oceanography and Fisheries, 1, 427–448.

EL-WAKEEL, S.K. and EL-SAYED, M.K., 1976. Preliminary investigation on the texture type of inner shelf sediments off Alexandria. Proceedings of Seminar on Nile Delta Shore Processes (With Emphasis on Hydrodynamical Factors). Alexandria: UNDP/UNESCO, 442–455.

EL-WAKEEL, S.K. and EL-SAYED, M.K., 1978. The texture, mineralogy and chemistry of bottom sediments and beach sands from the Alexandria region, Egypt. Marine Geology, 27, 137–160.

EL-WAKEEL, S.K. and WAHBY, S.D., 1970. Texture and chemistry of Lake Maryut sediments. Archiv fuer Hydrobiologie, 67(3), 368–395.

FAIRBANKS, R.G., 1989. A 17,000-year glacio-eustatic sea level record: Influence of glacial melting rates on the Younger Dryas event and deep-ocean circulation. Nature, 342, 637–642.

FOUCAULT, A. and STANLEY, D.J., 1989. Late Quaternary paleoclimatic oscillations in East Africa recorded by heavy minerals in the Nile delta. Nature, 339, 44–46.

FOURTAU, R., 1893. La région de Maryut; étude géologique. Bulletin de l'Institut d'Egypte, sèr. III, 4, 141.

FOURTAU, R., 1896. Les puits artésiens et les puits forés en Egypte. Bulletin de l'Institut d'Egypte, 7, 239–255.

FOURTAU, R., 1915. Contribution à l'étude des dépôts Nilotiques. Mémoires de l'Institut Egyptien, 8, 57–94.

FRIHY, O.E., 1992. Sea-level rise and shoreline retreat of the Nile delta promontories, Egypt. Natural Hazards, 5, 65–81.

FRIHY, O.E.; EL FISHAWI, M.M., and EL ASKARY, M.A., 1988. Geomorphological features of the Nile delta coastal plain: A review. Acta Adriatica, 29, 51–65.

FRIHY, O.E. and STANLEY, D.J., 1988. Texture and coarse fraction composition of Nile delta deposits: Facies analysis and stratigraphic correlation. Journal of African Earth Sciences, 7, 237–255.

GLENNIE, K.W., 1987. Desert sedimentary environments, present and past—a summary. Sedimentary Geology, 50, 135–165.

GUSTAVSON, T.C., 1991. Buried vertisols in lacustrine facies of the Pliocene Fort Hancock Formation, Hueco, west Texas and Chihuahua, Mexico. Geological Society of America Bulletin, 103, 448–460.

HAMROUSH, H.A. and STANLEY, D.J., 1990. Paleoclimatic oscillations in East Africa interpreted by analysis of trace elements in Nile delta sediments. Episodes, 13, 264–269.

HASSAN, F. A., 1981. Historical Nile floods and their implications for climatic change. Science, 212, 1142–1145.

HASSAN, F.A.; HEGAB, O., and EL-SHAHAT, A., 1986. Mediterranean littoral cycles, west Alexandria, Egypt and implications for archeological exploration. Nyame Akuma, 27, 3–5.

HASSOUBA, A.H., 1980. Quaternary sediments from the coastal plain of northwestern Egypt (from Alexandria to El-Omayid). Ph.D. Thesis, Univ. of London, London, 320p.

HASSOUBA, H. and SHAW, H.F., 1980. The occurrence of palygorskite in Quaternary sediments of the coastal plain of north-west Egypt. Clay Minerals, 15, 77–83.

HEY, R.W., 1978. Horizontal Quaternary shorelines of the Mediterranean. Quaternary Research, 10, 197–203.

HILMY, M.E., 1951. Beach sands of the Mediterranean coast of Egypt. Journal of Sedimentary Petrology, 21, 109–120.

HUME, W.F., 1912. The gypsum deposits of the Maryut region (a review). Cairo Scientific Journal, 6, 43–45.

HUME, W.F. and HUGHES, F., 1921. The Soils and Water Supply of the Maryut District, West of Alexandria. Cairo: Ministry of Finance, Survey of Egypt, 52p.

HUME, W.F. and LITTLE, O.H., 1928. Raised beaches and terraces of Egypt. Union de Géographie International (Report of the Commission on Pliocene and Pleistocene Terraces), Paris, 9–15.

INMAN, D.L. and JENKINS, S.A., 1984. The Nile littoral cell and man's impact on the coastal zone of the southeastern Mediterranean. Scripps Institution of Oceanography, Reference Series, 31, 1–43.

ISMAIL, M.M. and SELIM, A.A., 1969. Stratigraphy of the Salum area, Western Desert, U.A.R. Bulletin of the Faculty of Science, Alexandria University, 9, 309–330.

IWACO, Consultants for Ground Water and Environment, 1989. Landsat Thematic Mapper for hydrogeological mapping in Egypt. Report bcrs 89-28, Final report CO-1.7, Development and Management of Groundwater Resources in the Nile Valley and Delta Project, Rotterdam, Netherlands, 50p.

JACOTIN, P.M., 1818, Carte Topographique de l'Egypte et de Plusieurs Parties des Pays Limitrophes. Paris, 47 plates.

JONDET, M.G., 1916. Les ports submergés de l'ancienne

île de Pharos. *Mémoires de l'Institut Egyptien*, 9, 101p.

KERAMBRUN, P., 1986. Coastal lagoons along the southern Mediterranean coast (Algeria, Egypt, Libya, Morocco, Tunisia): Description and bibliography. *UNESCO Reports in Marine Sciences*, 34, 184p.

KULYK, V.A., 1987. Holocene foraminifera of the eastern Nile Delta, Egypt. M.Sc. Thesis, George Washington Univ., Washington, 90p.

LIGHTY, R.G.; MACINTYRE, I.G., and STUCKENRATH, R., 1982. Acropora palmata reef framework: A reliable indicator of sea level in the western Atlantic for the past 10,000 years. *Coral Reefs*, 1, 125–130.

LOIZEAU, J.-L. and STANLEY, D.J., in press. Petrological-statistical approach to interpret sub-recent lagoon subfacies, Idku, Nile delta of Egypt. *Marine Geology*.

MALDONADO, A. and STANLEY, D.J., 1979. Depositional patterns and late Quaternary evolution of two Mediterranean submarine fans: A comparison. *Marine Geology*, 31, 215–250.

MEDIBA (Mediterranean Basin Program), 1992. Nile Delta Project data-base listings. *Records, U.S. National Museum of Natural History*, Washington, D.C.

MITWALLY, H., 1982. Review of industrial wastewater disposal in Alexandria. *In: Proceedings of the International Symposium on Management of Industrial Wastewater in Developing Nations*, Alexandria, Egypt, 72–78.

MORCOS, S.A., 1985. Submarine archaeology and its future potential: Alexandria casebook. *In:* Richardson, J.G. (ed.), *Managing the Ocean.* Mount Airy, Maryland: Lomond Publishing, pp. 193–211.

MÖRNER, N.A., 1976. Eustatic changes during the last 8000 years in view of radiocarbon calibration and information from the Kattegutt region and other northwestern coastal areas. *Palaeogeography, Palaeoclimatology, Palaeoecology*, 19, 63–85.

NAFAS, M.G.; FANOS, A.M., and ELGANAINY, M.A., 1991. Characteristics of waves off the Mediterranean coast of Egypt. *Journal of Coastal Research*, 7, 665–676.

NEEV, D.; BAKLER, N., and EMERY, K.O., 1987. *Mediterranean Coasts of Israel and Sinai: Holocene Tectonism from Geology, Geophysics and Archaeology.* New York: Taylor & Francis, 130p.

NEEV, D.; GREENFIELD, L., and HALL, J.K., 1985. Slice tectonics in the eastern Mediterranean basin. *In:* Stanley, D.J. and Wezel, F.-C. (eds.), *Geological Evolution of the Mediterranean Basin.* New York: Springer-Verlag, pp. 249–269.

NEEV, D.; HALL, J.K., and SAUL, J.M., 1982. The Pelusium megashear system across Africa and associated lineament systems. *Journal of Geophysical Research*, 87(B2), 1015–1030.

NEWBERRY, P.E., 1908. The petty-kingdom of the Harpoon and Egypt's earliest Mediterranean port. *University of Liverpool Annals of Archaeology and Anthropology*, 1, 17–22.

OLIVER, F.W., 1945. Dust-storms in Egypt and their relation to the war period, as noted in Maryut, 1939–45. *The Geographical Journal*, 106, 27–49.

OLIVER, F.W., 1946. Dust-storms in Egypt as noted in Maryut: A supplement. *The Geographic Journal*, 108, 221–226.

PAULISSEN, E. and VERMEERSCH, P.M., 1989. Behaviour of large allogenous river systems: The example of the Saharan River Nile during late Quaternary. *Bulletin de la Société Géologique de France*, 5, 73–83.

PAVER, G.L. and PRETORIUS, D.A., 1954. Report on reconnaissance hydrogeological investigations in the Western Desert coastal zone. *Publication de l'Institut du Désert d'Egypte*, 5, 1–145.

PETIT-MAIRE, N., 1989. Interglacial environments in presently hyperarid Sahara: Palaeoclimatic implications. *In:* Leinen, M. and Sarnthein, N. (eds.), *Paleoclimatology and Paleometeorology: Modern and Past Patterns of Global Atmospheric Transport.* New York: Kluwer Academic, pp. 637–661.

PHILIP, G., 1976. Morphology of the Mediterranean coastal area between Rosetta and Sallum, Egypt. *Proceedings of Seminar on Nile Delta Sedimentology.* UNDP/UNESCO and University of Alexandria, Alexandria, pp. 25–32.

PICARD, L., 1943. Structures and evolution of Palestine. *Bulletin of the Geological Department Hebrew University, Jerusalem*, 4, 134p.

PIMMEL, A. and STANLEY, D.J., 1989. Verdinized fecal pellets as indicators of prodelta and delta-front deposits in the Nile delta, Egypt. *Marine Geology*, 86, 339–347.

PIRAZZOLI, P.A., 1987. Sea-level changes in the Mediterranean. *In:* Tooley, M.J. and Shennan, I. (eds.), *Sea-level Changes*, Institute of British Geographers, Special Publication, Series 20. Oxford, England: Basil Blackwell, pp. 152–181.

PIRAZOLLI, P.A., 1992. *World Atlas of Sea-level Changes.* Amsterdam: Elsevier Oceanography Series, 58, 300p.

PUGLIESE, N. and STANLEY, D.J., 1991. Ostracods, depositional environments and Late Quaternary evolution of the eastern Nile delta, Egypt. *Il Quaternario*, 4, 275–302.

REINECK, H.E. and SINGH, I.B., 1980. *Depositional Sedimentary Environments.* Berlin: Springer-Verlag, 549p.

RIEHL, H. and MEITIN, J., 1979. Discharge of the Nile River: A barometer of short-period climatic variations. *Science*, 206, 1178–1179.

RODZIEWICZ, M., 1984. *Les habitations romaines tardives d'Alexandrie à la lumière des fouilles polonaises à Kôm El-Dikka.* Warsaw: PWN-Editions Scientifique de Pologne, 443p.

SAAD, M.A.H., 1972. Effect of pollution on the sediments of Lake Mariut, Egypt. *Rapport de la Commission Internationale pour l'Exploration de la Mer Méditerranée*, 21.3, 125–127.

SAAD, M.A.H., 1980. Characteristics of sediments from three different water bodies surrounding Alexandria. *Bulletin de l'Office National des Pêcheries de Tunisie*, 4, 273–282.

SAAD, M.A.H., 1983a. Influence of pollution on Lake Mariut, Egypt: I. Environmental characteristics. *Rapport de la Commission Internationale pour l'Exploration de la Mer Méditerranée*, 28.6, 207–208.

SAAD, M.A.H., 1983b. Influence of pollution on Lake Mariut, Egypt: II. Nutrients. *Rapport de la Commission Internationale pour l'Exploration de la Mer Méditerranée*, 28.6, 209–210.

SAAD, M.A.H.; ABU ELAMAYEM, M.M.; EL-SEBAE, A.H., and SHARAF, I.F., 1982. Occurrence and distribution of chemical pollutants in Lake Mariut, Egypt: I. Res-

idues of organochloride pesticides. *Water, Air and Soil Pollution,* 16, 245–252.

SAAD, M.A.H.; EL-RAYIS, O.A., and AHDY, H.H., 1984. Status of nutrients in Lake Mariut, a delta lake in Egypt suffering from intensive pollution. *Marine Pollution Bulletin,* 15, 408–411.

SAAD, M.A.H.; EZZAT, A.A.; EL-RAYIS, O.A., and HAFEZ, H., 1981. Occurrence and distribution of chemical pollutants in Lake Mariut, Egypt. II. Heavy metals. *Water, Air, and Soil Pollution,* 16, 401–407.

SAAD, M.A.H.; McCOMAS, S.R., and EISENREICH, S.J., 1985. Metals and chlorinated hydrocarbons in surficial sediments of three Nile delta lakes, Egypt. *Water, Air, and Soil Pollution,* 24, 27–39.

SAID, R., 1981. *The Geological Evolution of the River Nile.* New York: Springer-Verlag, 151p.

SAID, R.; PHILIP, G., and SHUKRI, N.M., 1956. Post Tyrrhenian climatic fluctuations in northern Egypt. *Quaternaria,* 3, 167–172.

SANDFORD, K.S. and ARKELL, W.J., 1939. Paleolithic man and the Nile Valley in lower Egypt. *Chicago University, Oriental Institute Publication,* 36, 1–105.

SCHWEGLER, E., 1948. Vorgänge subaerischer diagenese in Küstendünensanden des ägyptischen Mittelmeer-Gebiets. *Neues Jahrbuch fuer Mineralogie, Geologie, und Palaontologie. Montashefte,* Abt. B, H.1–4, 9–16.

SESTINI, G., 1989. Nile delta: A review of depositional environments and geological history. *In:* Whateley, M.G.K. and Pickering, K.T. (eds.), *Deltas: Sites and Traps for Fossil Fuels.* Geological Society of London, Special Publication, 41, 99–127.

SHAFEI, A., 1952. Lake Mareotis—its past history and its future development. *Bulletin de l'Institut Fouad I du Désert,* 2(1), 71–101.

SHARAF EL DIN, S.H., 1977. Effect of the High Aswan Dam on the Nile flood and on estuarine and coastal circulation along the Mediterranean Egyptian coast. *Limnology and Oceanography,* 22, 194–207.

SHATA, A., 1955. An introductory note on the geology of the northern portion of the Western Desert of Egypt. *Bulletin de l'Institut du Désert d'Egypte,* 5, 96–106.

SHATA, A., 1958. Remarks on the physiography of the El-Airia–Maryut area. *Bulletin de la Société Géographique d'Egypte,* 30, 53–74.

SHUKRI, N.M., 1950. The mineralogy of some Nile sediments. *Quaternary Journal of the Geological Society of London,* 105, 511–534.

SHUKRI, N.M. and PHILIP, G., 1955. The geology of the Mediterranean coast between Rosetta and Bardia, Part I, recent sediments: Mechanical analysis and mineral composition. *Bulletin de l'Institut d'Egypte,* 36, 445–465.

SHUKRI, N.M.; PHILIP, G., and SAID, R., 1956. The geology of the Mediterranean coast between Rosetta and Bardia, Part II, Pleistocene sediments: Geomorphology and microfacies. *Bulletin de l'Institut d'Egypt,* 37, 395–427.

SHUKRI, N.M. and PHILIP, G., 1956. The geology of the Mediterranean coast between Rosetta and Bardia, Part III, Pleistocene sediments: Mineral analysis. *Bulletin de l'Institut d'Egypte,* 37, 445–455.

STANLEY, D.J., 1988. Subsidence in the northeastern Nile delta: Rapid rates, possible causes and consequences. *Science,* 240, 497–500.

STANLEY, D.J., 1989. Sediment transport on the coast and shelf between the Nile delta and Israeli margin as determined by heavy minerals. *Journal of Coastal Research,* 5, 813–828.

STANLEY, D.J., 1990. Recent subsidence and northeast tilting of the Nile delta, Egypt. *Marine Geology,* 94, 147–154.

STANLEY, D.J. and CHEN, Z., 1991. Distinguishing sand facies in the Nile delta, Egypt, by stained grain and compositional component analysis. *Journal of Coastal Research,* 7, 363–377.

STANLEY, D.J. and HAMZA, F.H., 1992. Terrigenous-carbonate sediment interface (Late Quaternary) along the northwestern margin of the Nile delta, Egypt. *Journal of Coastal Research,* 8, 153–171.

STANLEY, D.J.; WARNE, A.G.; DAVIS, H.R.; BERNASCONI, M.P., and CHEN, Z., 1992. Late Quaternary evolution of the north-central Nile delta between Manzala and Burullus lagoons, Egypt. *National Geographic Research & Exploration,* 8, 22–51.

STOFFERS, P.; SUMMERHAYES, C.P., and DOMINIK, J., 1980. Recent pelletoidal carbonate sediments off Alexandria, Egypt. *Marine Geology,* 34, M1–M8.

SUMMERHAYES, C.P.; SESTINI, G.; MISDORP, R., and MARKS, N., 1978. Nile Delta: Nature and evolution of continental shelf sediments. *Marine Geology,* 27, 43–65.

TOUSSOUN, O., 1922. Mémoires sur les anciennes branches du Nil Époque Ancienne. *Mémoire de l'Institut d'Egypte,* 4, 212p.

TOUSSOUN, O., 1934. Les ruines sous-marines de la Baie d'Aboukir. *Bulletin de la Société Royale d'Archéologie, Alexandrie,* 29, 342–352.

UNDP/UNESCO, 1976. *Proceedings of Seminar on Nile Delta Sedimentology.* Alexandria: UNDP, 257p.

UNDP/UNESCO, 1977. *Proceedings of Seminar on Nile Delta Shore Processes.* Alexandria: UNDP, 624p.

UNDP/UNESCO, 1978. *Coastal Protection Studies. Project Findings and Recommendations.* UNDP/EGY/73/063, Paris, 483p.

U.S. DEFENSE MAPPING AGENCY, 1961. Sheet 5287.1, Series P773, Edition 1-AM3 (scale—1:50,000).

U.S. DEFENSE MAPPING AGENCY, 1973, Sheets 5186.1, Series P773, Edition 2-DMATC (scale—1:50,000).

U.S. DEFENSE MAPPING AGENCY, 1975, Sheets 5286.1, 5286.4, Series P773, Edition 2-DMATC (scale—1:50,000).

U.S. DEFENSE MAPPING AGENCY, 1977, Sheets 5287.2, 5287.3, 5386.4, 5387.3, 5387.4, Series P773, Edition 3-DMA (scale—1:50,000).

U.S. DEFENSE MAPPING AGENCY, 1985. *Mediterranean Sea: El Iskandarîya to the Sinai.* Map 56100 (scale—1:50,000).

U.S. DEFENSE MAPPING AGENCY, 1990. *Mediterranean Sea: Approaches to El-Iskandariya including Sîdi Karir and Abû Qîr.* Map 56101 (scale—1:50,000).

WAHBY, S.D. and ABDEL MONEIM, M.A., 1979. The problem of phosphorus in the eutrophic Lake Maryût. *Estuarine and Coastal Marine Science,* 9, 615–622.

WAHBY, S.D. and ABDEL MONEIM, M.A., 1983. Inorganic nitrogen compounds and nitrogen load in the eutrophic Lake Maryut. *Rapport de la Commission Internationale pour l'Exploration de la Mer Méditerranée,* 28.6, 201–202.

WAHBY, S.D.; KINAWY, S.M.; EL-TABBACH, T.I., and AB-

DEL MONEIM, M.A., 1978. Chemical characteristics of Lake Maryût, a polluted lake south of Alexandria, Egypt. *Estuarine and Coastal Marine Science,* 7, 17–28.

WATERBURY, J., 1979. *Hydropolitics of the Nile Valley.* Syracuse, New York: Syracuse University Press, 301p.

WEST, I.M.; ALI, Y.A., and HILMY, M.E., 1979. Primary gypsum nodules in a modern sabkha on the Mediterranean coast of Egypt. *Geology,* 7, 354–358.

WILGUS, C.K.; HASTINGS, B.S.; KENDALL, C.G.ST.C.; POSAMENTIER, H.W.; ROSS, C.A., and VAN WAGONER, J.C. (eds.), 1988. *Sea-Level Changes: An Integrated Approach.* Society of Economic Paleontologists and Mineralogists, Special Publication 42, 306p.

ZEUNER, F.E., 1952. Pleistocene shore-lines. *Geologische Rundschau,* 40, 39–50.